AD_____

Award Number: DAMD17-99-1-9065

TITLE: Magnetic Resonance Studies of Photosensitizers and their Effect in Tumors

PRINCIPAL INVESTIGATOR: Subbaraya Ramaprasad, Ph.D.

CONTRACTING ORGANIZATION: University of Nebraska Medical Center
Omaha, Nebraska 68198-5100

REPORT DATE: August 2002

TYPE OF REPORT: Annual

PREPARED FOR: U.S. Army Medical Research and Materiel Command
Fort Detrick, Maryland 21702-5012

DISTRIBUTION STATEMENT: Approved for Public Release;
Distribution Unlimited

REPORT DOCUMENTATION PAGE

Form Approved
OMB No. 074-0188

1. AGENCY USE ONLY (Leave blank)	2. REPORT DATE	3. REPORT TYPE AND DATES COVERED
	August 2002	Annual (15 Jul 01 - 14 Jul 02)

4. TITLE AND SUBTITLE
Magnetic Resonance Studies of Photosensitizers and their Effect in Tumors

5. FUNDING NUMBERS
DAMD17-99-1-9065

6. AUTHOR(S)
Subbaraya Ramaprasad, Ph.D.

7. PERFORMING ORGANIZATION NAME(S) AND ADDRESS(ES)
University of Nebraska Medical Center
Omaha, Nebraska 68198-5100

E-Mail: SRAMAPRASAD@UNMC.EDU

8. PERFORMING ORGANIZATION REPORT NUMBER

9. SPONSORING / MONITORING AGENCY NAME(S) AND ADDRESS(ES)
U.S. Army Medical Research and Materiel Command
Fort Detrick, Maryland 21702-5012

10. SPONSORING / MONITORING AGENCY REPORT NUMBER

11. SUPPLEMENTARY NOTES
report contains color

12a. DISTRIBUTION / AVAILABILITY STATEMENT
Approved for Public Release; Distribution Unlimited

12b. DISTRIBUTION CODE

13. ABSTRACT ***(Maximum 200 Words)***
The main goal of this project is to study the fluorine labeled photosensitizers in the treatment of tumor models of relevance to breast cancer by photodynamic therapy. This study will use ^{19}F MR spectroscopy to determine the accumulation of photosensitizers in the tumor mass and the time at which maximum accumulation occurs in the tumor. Tumor destruction is achieved via appropriate laser irradiation when there is maximum amount of photosensitizer in the tumor volume. The rate of absorption and the peak times will be obtained to perform photodynamic therapy(PDT) studies involving the labeled photosensitizers. In vivo Phosphorous-31 NMR will be utilized before and after initiation of PDT to determine the effectiveness of this spectroscopic technique in predicting PDT outcome. Finally the ^{1}H MR diffusion imaging will be performed at several time points post PDT treatment to obtain a complete picture of tumor necrosis and tissue viability. The combined use of the multinuclear techniques on tumor model can provide significant information towards breast cancer treatment by PDT.

14. SUBJECT TERMS	15. NUMBER OF PAGES
breast cancer, photodynamic therapy (PDT), ^{19}F NMR, ^{31}P NMR, relaxation time, diffusion imaging, RF coils	59
	16. PRICE CODE

17. SECURITY CLASSIFICATION OF REPORT	18. SECURITY CLASSIFICATION OF THIS PAGE	19. SECURITY CLASSIFICATION OF ABSTRACT	20. LIMITATION OF ABSTRACT
Unclassified	Unclassified	Unclassified	Unlimited

Table of Contents

INTRODUCTION

The diagnosis and treatment of cancer is an important healthcare issue. This project is concerned with the development and monitoring of fluorine labeled photosensitizer for the treatment of breast cancer. The photosensitizers are new and hence can not be administered to humans directly. This necessitates the use of a suitable tumor model. Using a mouse foot tumor model, we will monitor the photosensitizer, obtain the rate of absorption and the time of maximum absorption which will be used to irradiate the tumor with appropriate laser. The response to PDT will be measured via the use of P-31 MR spectroscopy and 1H MR diffusion imaging techniques. These studies will provide information of significant value to breast cancer research and treatment.

Body (Research accomplishments)

Task-1

As a significant part of the study we have been able to obtain fluorinated photosensitizer with 12 equivalent fluorine atoms in the porphyrin photosensitizer. The structure and the details of the synthesis are provided in the appendix(pages 7-8) This form of the photosensitizer was tested by the Co-I at Roswell Park cancer Institute (Buffalo New York) in Radiation induced fibrosarcoma (RIF) cells and found to be a n effective photosensitizer. This sensitizer has an absorption peak at 626nm and is effective at 5-micromole concentration. Further details are provided in the manuscript (in preparation) and is also included as part of the Appendix at the end.

Task-2

This work was started in early November with the basic work being done by a part time student in a neighboring university. After gaining experience in maintaining the cell lines such as SKBR3 and MRA231 breast cancer cells, we moved on to growing and maintaining the RIF cells for the present project following the protovol of Twentyman et al (1). We have grown a number of tumors in foot and the flank. We have followed the unperturbed growth of these tumors and the growth charts for each of the tumors studied are provided in the Appendix (pages 9-10). Typical tumors grown on the foot and flank are shown in photographs (see pages 11-12 in Appendix) which follow the tumor growth charts.

Magnetic resonance studies

The relaxivity of unperturbed tumors were measured on our 7T MR imaging system. The T2 measurements were done by generating the multi-slice multi echo sequence providing images at different echo times. The regions of interest were selected from a representative image(see page 13, appendix)and the T2 values were computed for these regions in the tumor volume. The average T2 value was found to be 56±8 ms for the flank tumor and the corresponding T2 from elsewhere in the abdomen region was 37±7 ms. Similarly the T1 values were ~1.6 ±0.2 s and 1.2±0.2 s for the tumor and the abdomen regions. An inspection of the images did not reveal any visible necrotic regions in these unperturbed tumors.The appearance of necrotic regions in the tumors have been observed by other investigators in the T2 weighted images (2,3). The changes in T1 and or T2 values with the initiation of PDT treatment can provide more information on the possible mechanism of action of photosensitizer and their effect in tumor micro environment(4). The photosensitizer (which we call DoD-2) and the corresponding nonfluorinated analog were prepared as 1% tween solutions at Roswell park Cancer Institute as they do not dissolve in water. The concentration of these drugs in the solution was determined using known extinction coefficient and the absorptivity at 500nm. The concentrations of Dod-1 and DoD-2 are 356 and 275μM respectively.

A series of ^{19}F MR spectra were collected on our 7T instrument using a home built 1.5cm diameter coil. This coil can be tuned to both ^{1}H and ^{19}F frequency allowing the image and spectroscopic data to be collected from the tumor volume without disturbing the animal. The coil descriptions and the photographs of the coil assembly is shown in the Appendix(page 14).

The spectra that were recorded at different dilutions indicate that a low concentration corresponding to 30μg of DoD–2 can be detected at a high signal to noise ration in about 1 hour of data collection (The ^{19}F MR spectrum is shown in page 15).

In vivo ^{19}F MR studies: In vivo MR studies were performed using DoD-2 on mice bearing a foot tumor and one that does not have tumor. We performed studies on blood drawn after 1 hr of injection and also on the foot tumor a series of spectral data were collected

After administering the fluorine labeled DoD-2. We were not successful in obtaining any fluorine spectrum in about 2 hours of data collection. The possible reasons are that the drug administered is still very low in concentration. Since the mouse weighed about 21 gm and the drug administered was approximately 0.3 mg it leads to about about 15μg per gram of mouse. We have been successful in obtaining spectra at 30μg level in the pure solution state. We can expect the lines to be much broader and hence less sensitive to detection and quantitation. A single dose in the range of 1.5-2.5 mg of the compound should be able to provide significant signal. Other problems such the sparingly soluble form of the photosensitizer would add significantly to the sensitivity problem. We are now in the process of constructing the most water-soluble form with more fluorines to further enhance the sensitivity

The DoD-2 and dod1 are being studied in our laboratory for their photosensiting propertied and how P-31 MR can be used to assess the PDT responses and prognostic value in therapy involving such new photosensitizers. The saddle coil that resonantes at P-31 frequency for the 7T system has just been completed. A recent photograph has also been provided in the appendix (page 16).

We have been testing the PDT efficacy in the tumors involving the well-known FDA approved photosensitizer. More optimization studies are being done and this will be followed by studies involving DoD-1 and DoD-2 compounds.

KEY RESEARCH ACCOMPLISHMENTS;

1. Synthesis of fluorinated and its non-fluorinated analogs for PDT studies in sufficient quantity.

2. Construction of ^{1}H-^{19}F coil for studying the proton images and collecting ^{19}F spectra or images.

3. Growth and maintenance of RIF tumor on the flank and foot of male mice.

4. Study of unperturbed growth of several tumors in the flank and foot of mice.

5. Successful imaging of tumors using the Bruker volume coil and the home made proton surface coil

6. Successful mapping of spin lattice (T_1) and spin-spin (T_2) times in the RIF tumors. These studies will be pursued before and after PDT.

REPORTABLE OUTCOMES

1. We have enclosed a manuscript that will be submitted shortly. This should be considered as unpublished since it may take about 2 weeks before it goes to the Journal editor.

2. We have included a copy of the Abstract that was accepted for presentation at the ERA of Hope meeting at Orlando, September 25-28, 2002. (see page 17 on Appendix)

3. Development of two coils relevant to the project at the university of Nebraska medical Center (see Photographs in the Appendix).

CONCLUSIONS

Our results show that fluorinated photosensitizers can be produced in large enough quantities. These sensitizers can be detected at 7T field strength using a suitable 19F coil at a concentration of 30μg of the sample(eg. DoD2). More equivalent fluorines can significantly reduce the scan time and make it more practical at even lower concentrations. Additionally by producing these compounds in the water-soluble form, one can obtain higher quality spectral data which will further enhance the observation of the sensitizer in small volumes. We also have to increase the administered dose to the level of a 1-2 mg. Such studies are currently underway in our laboratory.

As a part of the entire project, we reported in the previous that the porphyrins with 6 fluorines,was being synthesized. The yield at the last step of the turned out to be too low and hence not practical to pursue the synthesis. Therefore, the strategy was changed y and synthesized porphyrins with 12 equivalent fluorines. This strategy also provides an opportunity to prepare symmetrical water soluble porphyrins and bacteriochlorins up to 24 fluorine atoms.

References

1. Twentyman PR, Brown JM, Gray JW, frank AJ, Scoles MA, Kallman RF. A new mouse tumor model system(RIF-1) for comparison of end point studies. J. Natl. cancer Inst., 1980, 64, 595-604.

2. Dodd NJF, Moore JV, Poppitt DG and Wood B. In vivo magnetic resonance imaging of the effects of Photodynamic therapy. Br. J. Cancer, 1989, 60, 164-167.

3. DeCertaines JD, Albrectsen J, larsen VA, Xie X, Rygaard J, Henricksen O, In vivo 31P magnetic resonance spectroscopy and 1H magnetic resonance Imaging of human bladder carcinoma on Nude Mice: Effects of Tumor growth and Treatment with cis-Dichloro –Diamine platinum. In Vivo, 1992, 6, 611-616.

4. Liu YH, Hawk RM, Ramaprasad S. In vivo relaxation time measurements on a murine tumor model—prolongation of T1 after photodynamic therapy. Magn. Reson. Imaging. 1995, 13, 251-258.

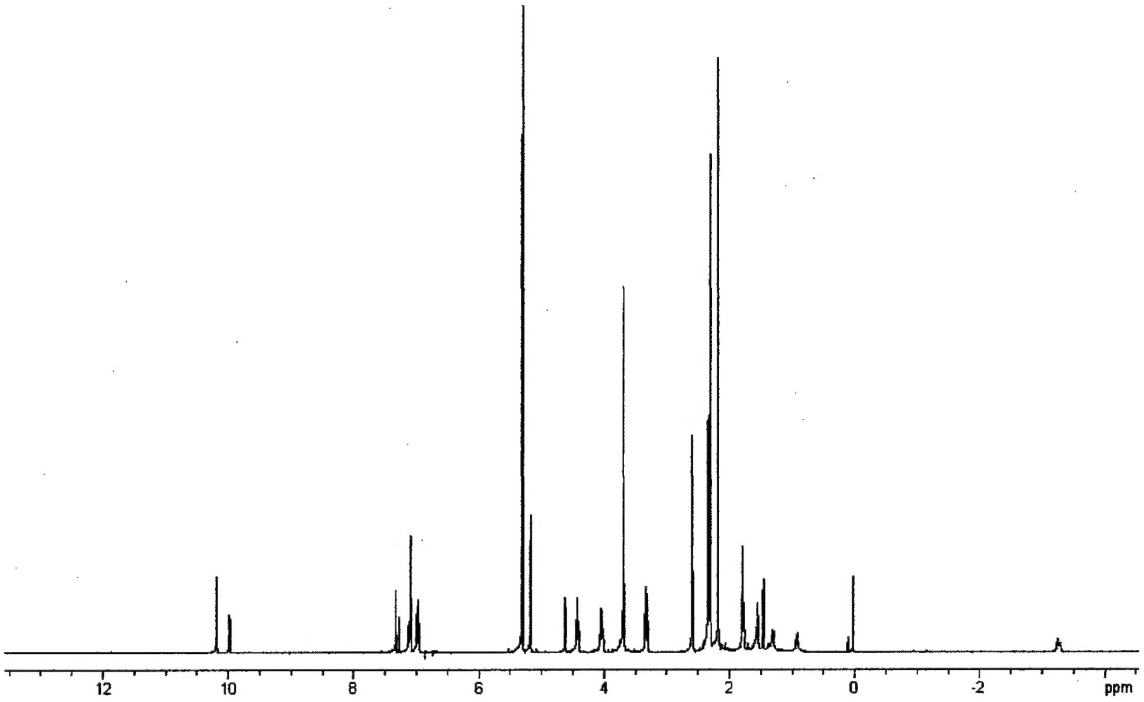

^{1}H-NMR Spectrum of 5-[{3,5-bis(3,5-dimethylbenzyloxy)phenyl}]-2,8-diethyl-13,17-bis(2-methoxycarbonylethyl)porphyrin in $CDCl_3$.

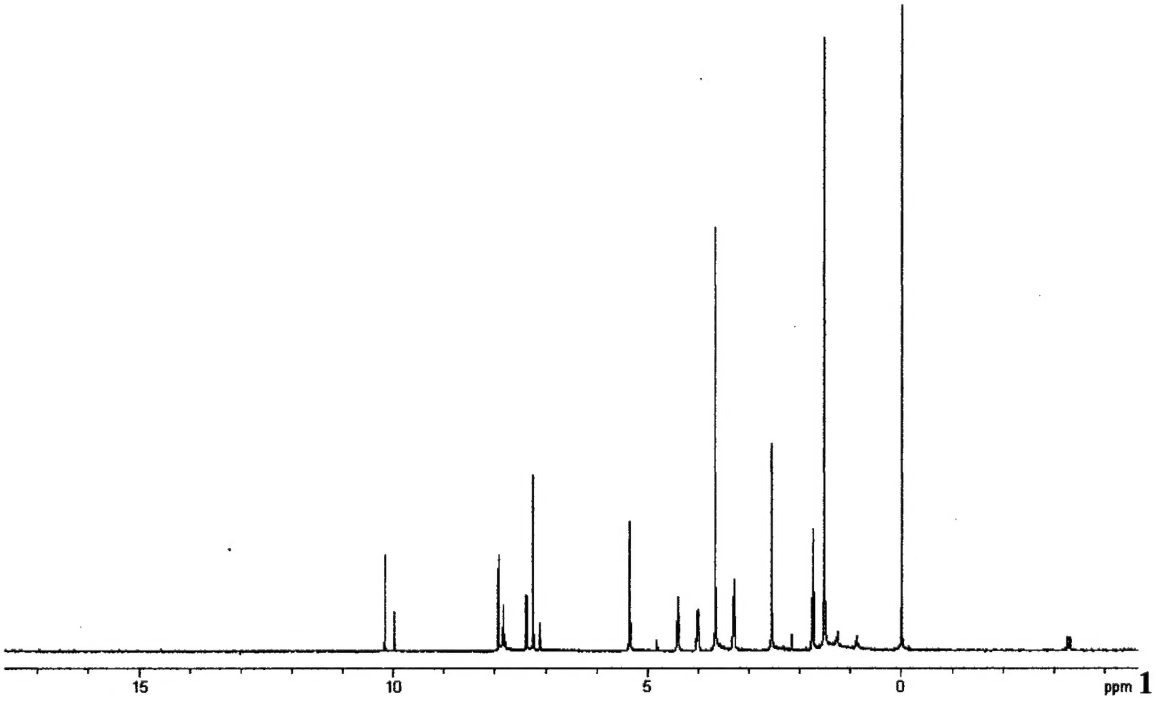

H-NMR Spectrum of 5-[3,5-bis{3,5-bis(triflurомethyl)benzyloxy}phenyl]-2,8-diethyl-13,17-bis(2-methoxycarbon

ylethyl)porphyrin in $CDCl_3$.

F-19 NMR Spectrum of Fluorinated Porphyrin

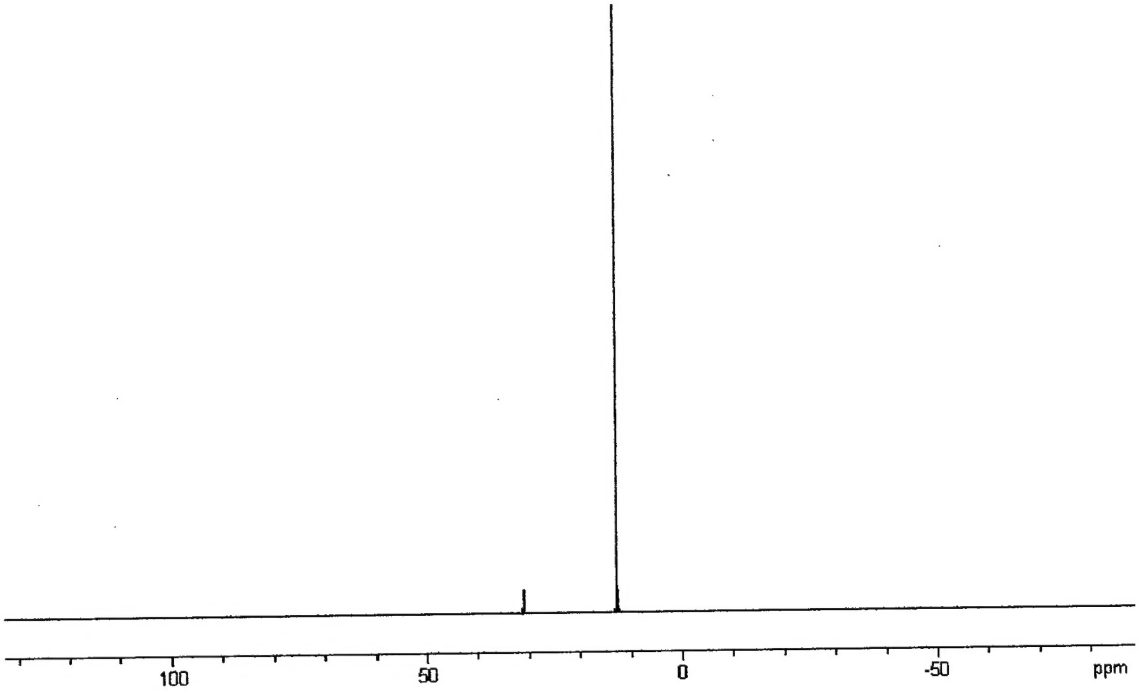

^{19}F-NMR Spectrum of 5-[3,5-bis{3,5-bis(trifluromethyl)benzyloxy}phenyl]-2,8-diethyl-13,17-bis(2-methoxycarbon ylethyl)porphyrin

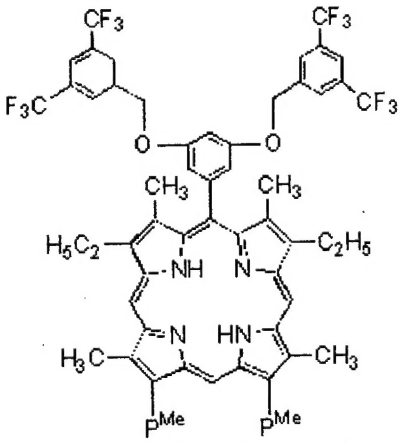

Fluorinated Porphyrin

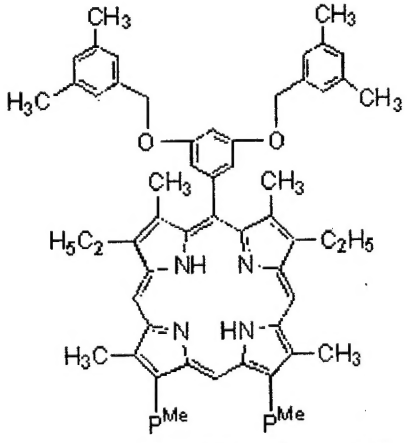

Non-Fluorinated Porphyrin

Mice tumor volumes on foot

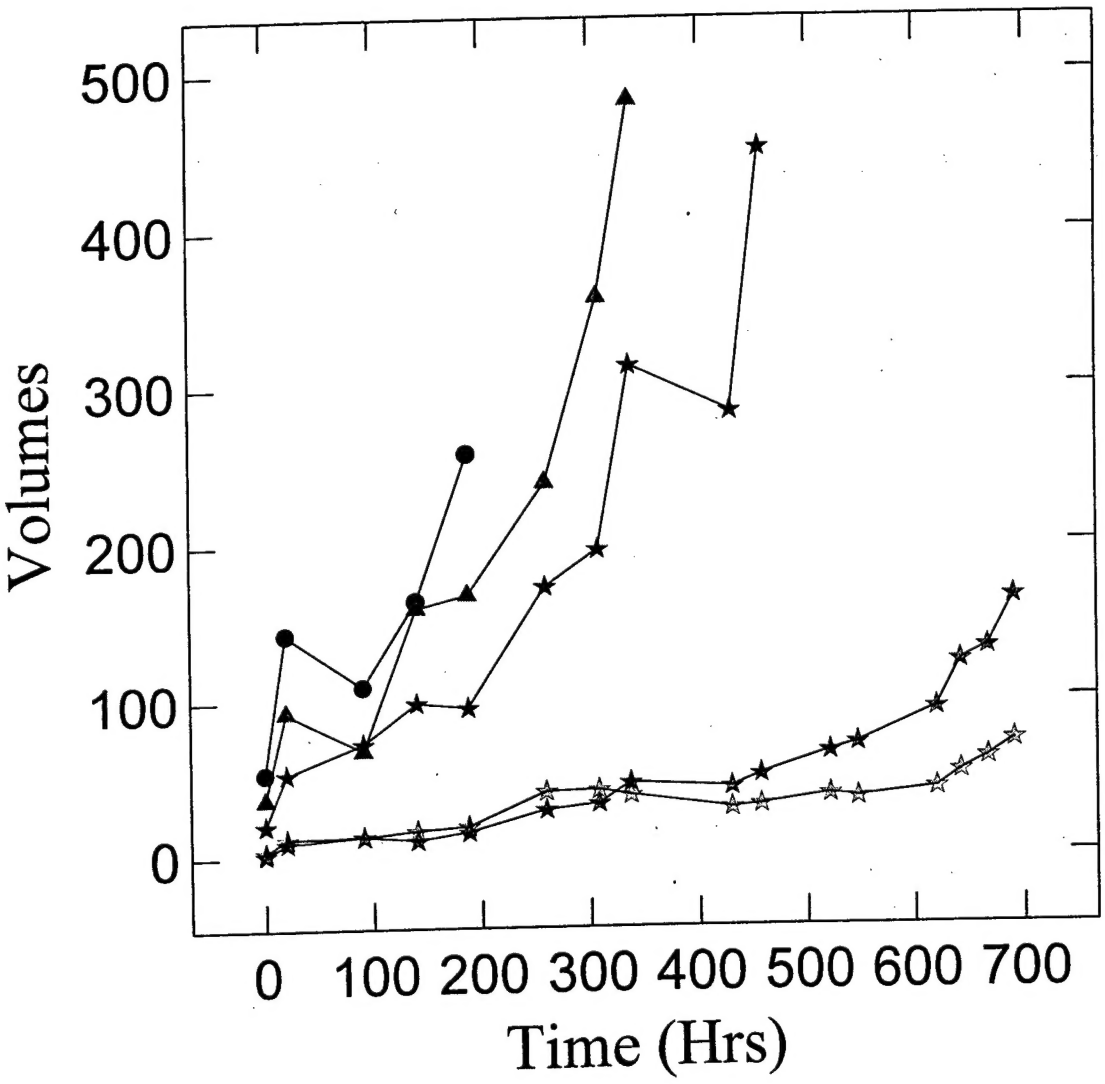

Mice tumor volumes on flank

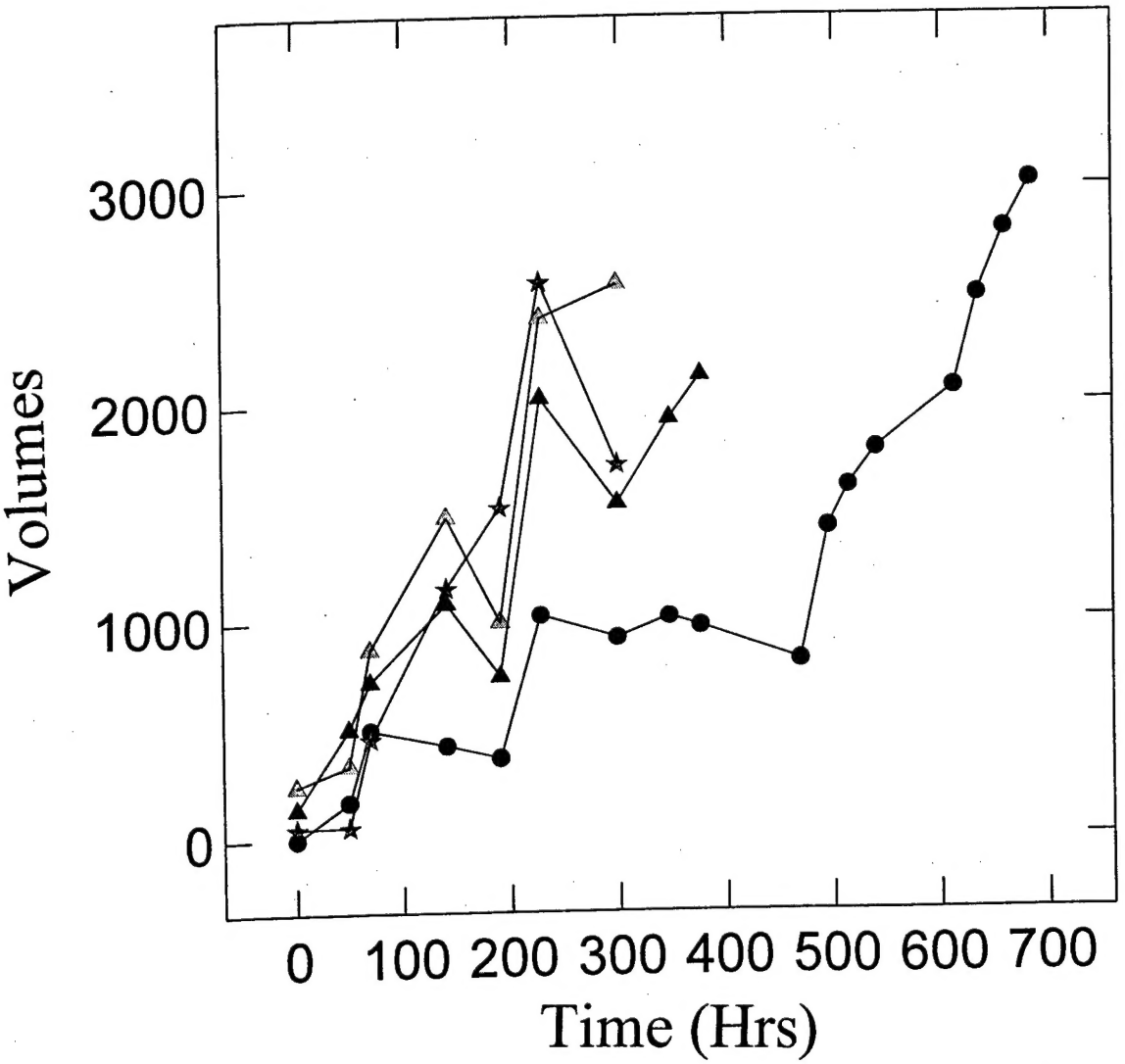

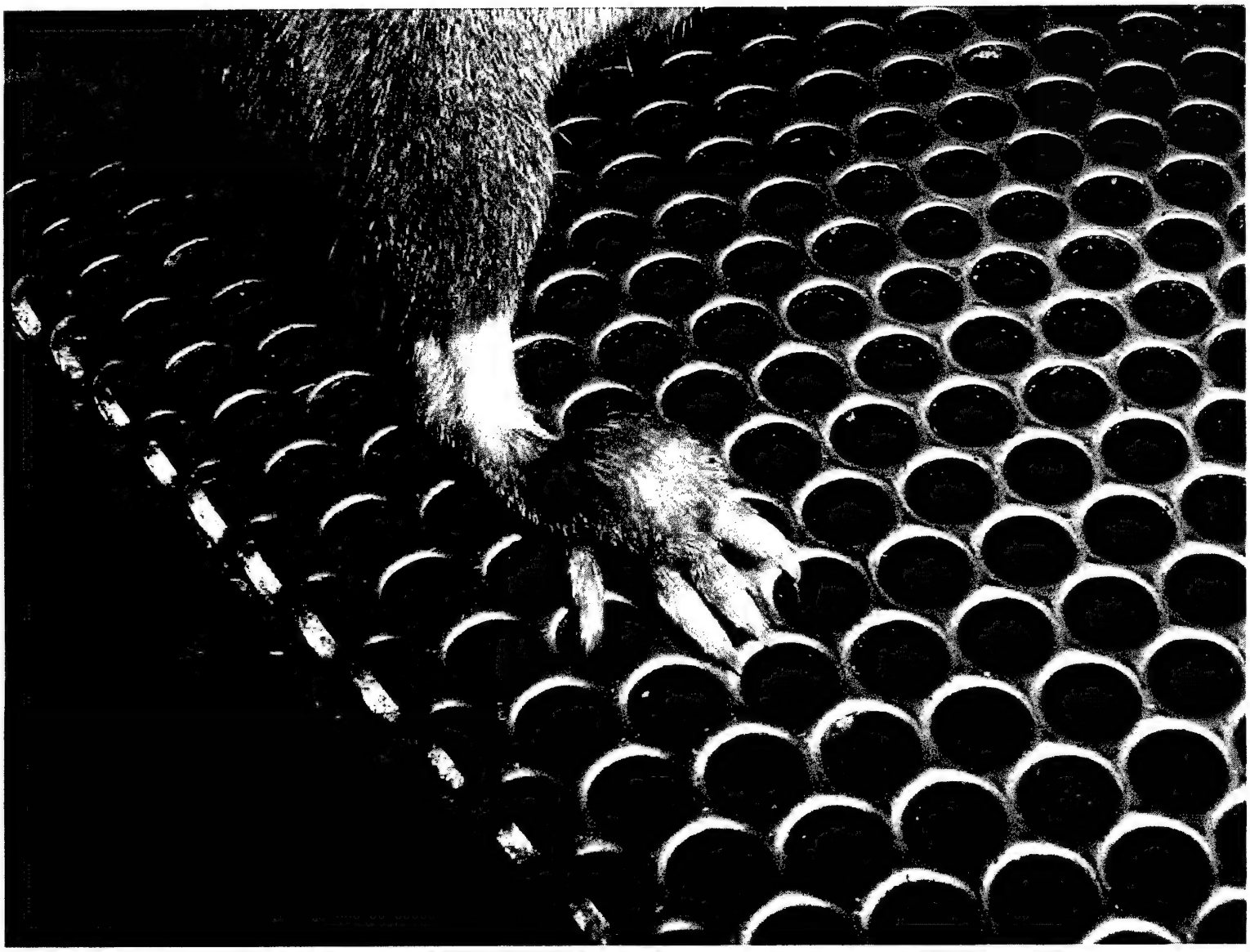

Photograph of a typical mouse foot bearing RIF-1 tumor grown in our laboratory.

Photograph of a typical RIF-1 tumor grown on mouse flank in our laboratory.

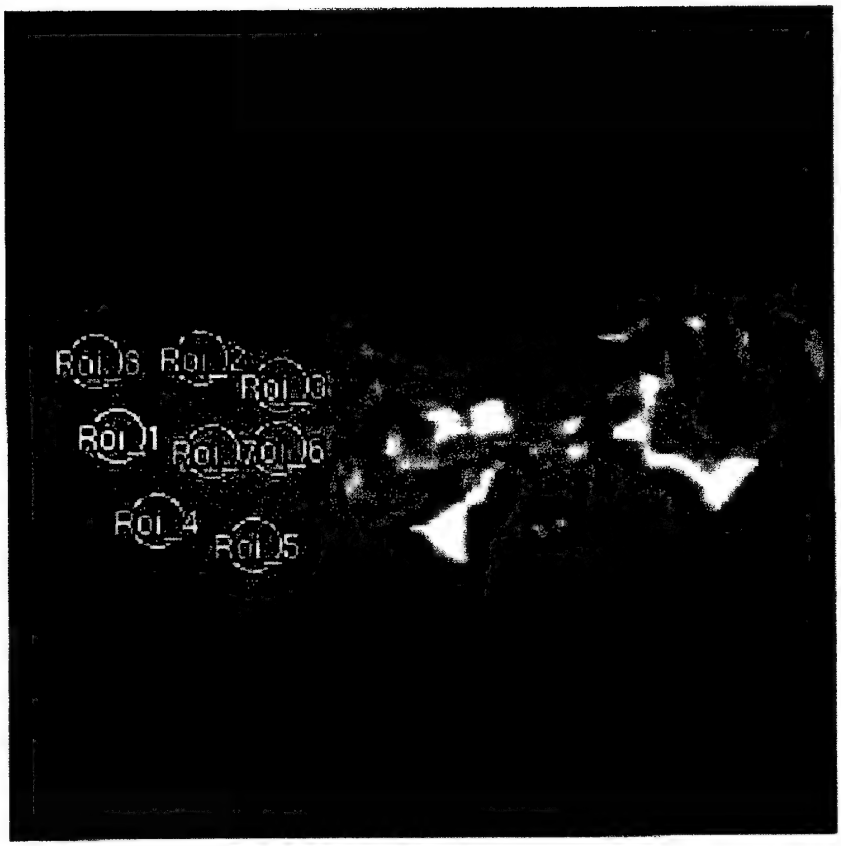

A spin echo image of 1mm slice through the mouse abdomen. The 8 regions of interest shown on the images were used to compute the relaxation times of water protons in the tumor mass.

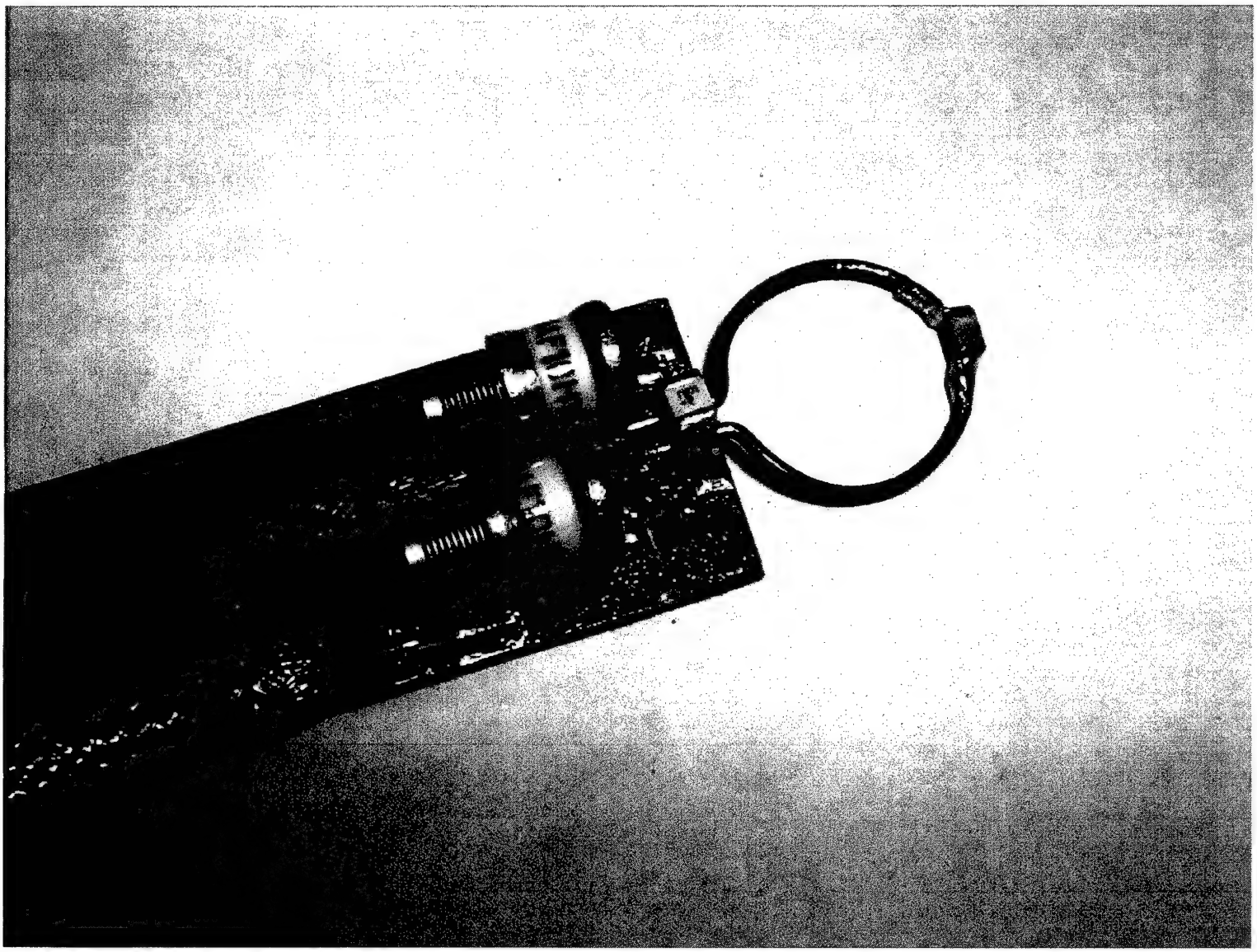

An RF surface coil (1.5 cm diameter) tunable to both ^{1}H and ^{19}F frequencies at 7 tesla.

A ^{19}F spectrum of 30μg of the newly synthesized DoD-2 recorded at 7T instrument

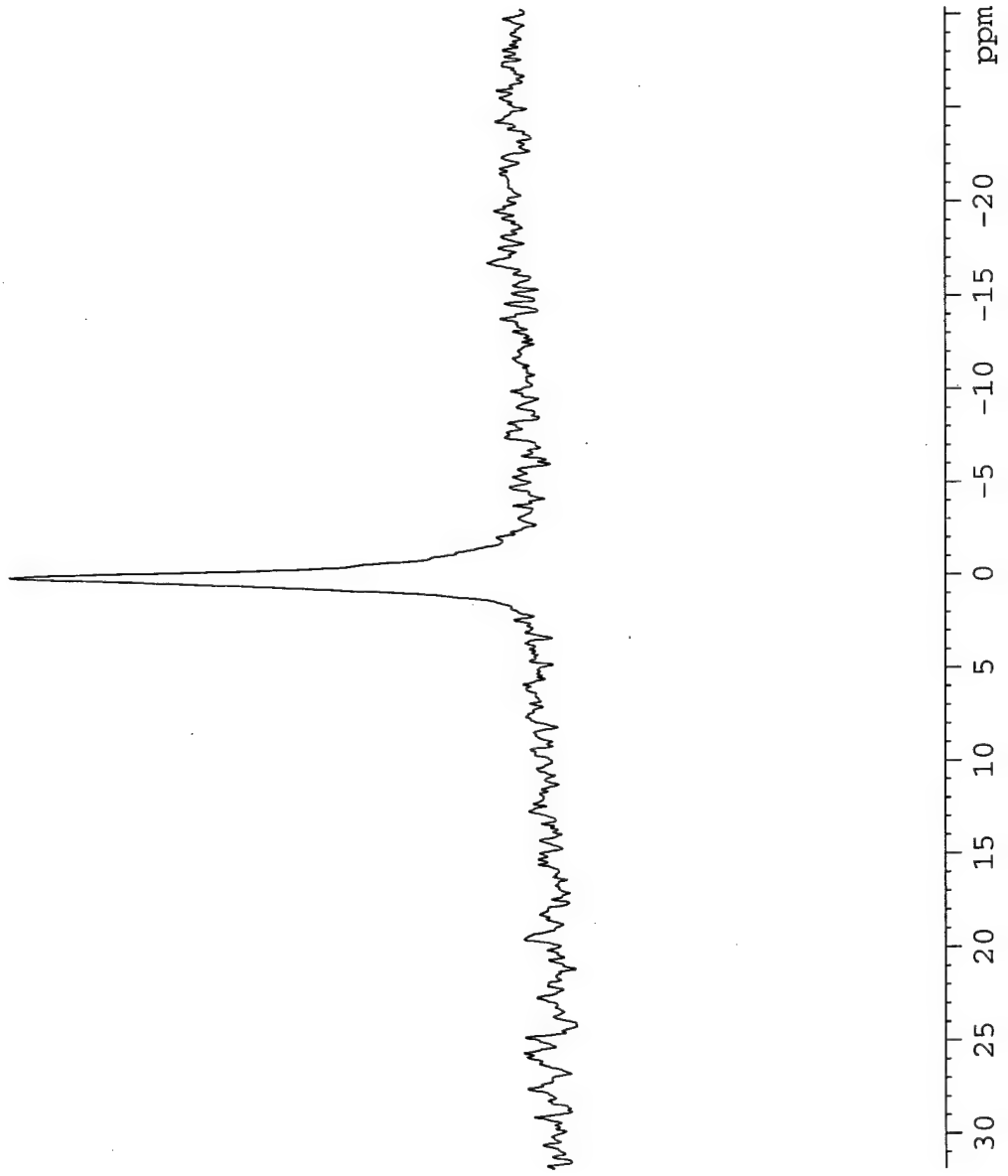

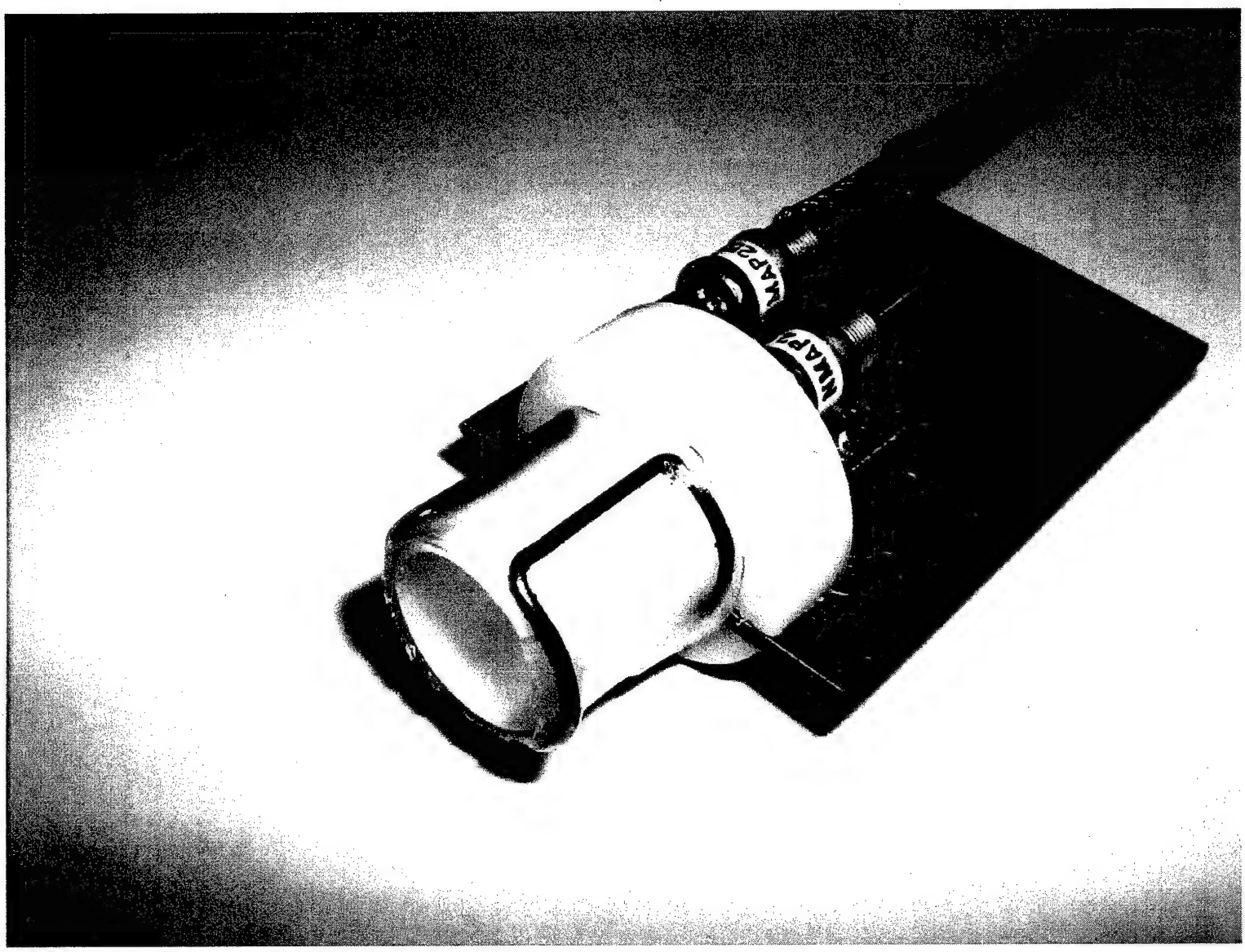

A Phosphorus –31 RF coil constructed in our laboratory for studying P-31 MR spectra of tumors. This is a saddle coil of 1.5cm diameter sufficient to accommodate foot tumors inside the coil.

Accepted for the 'Era of hope of Meeting' at Orlando, Florida, September 2002.

SYNTHESIS AND IN-VITRO PHOTOSENSITIZING EFFICACY OF FLUORINATED PORPHYRIN-BASED PHOTOSENSITIZERS FOR IN-VIVO MR STUDIES

Suresh K. Pandey, Amy L. Gryshuk, Andrew Graham, Allan Oseroff, S. Ramaprasad* and Ravindra K. Pandey

Photodynamic Therapy Center, Roswell Park Cancer Institute, Buffalo, NY 14263 and *Department of Radiology,Nebraska Medical Center, Omaha, NE 68198

Ravindra.pandey@Roswellpark.org and SRamaprasad@unmc.edu

ABSTRACT: In vivo MR spectroscopy has been used increasingly to monitor metabolism and disease states in humans. Both magnetic resonance imaging and spectroscopy have evolved into sophisticated diagnostic techniques. In addition to the proton, nuclei such as fluorine can be studied by in vivo spectroscopy and imaging. Fluorine-19 NMR is a technique with significant potential because of the relatively high sensitivity and low endogenous background. Fluorine-19 MR has been used to study metabolism, tumor growth, and blood flow. MR of fluorinated compound is particularly attractive for in vivo studies of human and animal models. The F-19 isotope has a 100% natural abundance, a spin of 1/2, and an MR sensitivity that is 83% that of hydrogen.

To date, most of the fluorinated porphyrin-based analogs synthesized for in-vivo F-19 NMR studies have been unsymmetrical, and thus lead to signal dispersion. In order to have strong fluorine signal at a low concentration of the drug in tumor, it is necessary to have photosensitizers containing multiple fluorine units. It would be advantageous to have a center of symmetry in the fluorinated photosensitizer that will render the fluorine nuclei to be equivalent and provide signal addition of all equivalent nuclei.We have succeeded in synthesizing porphyrins containing six to 12 symmetrical fluorines. These compounds were prepared in multi-step syntheses. The structures were confirmed by NMR , masspectrometry and elemental analyses. The symmetry of the fluorines was confirmed by F-19 NMR studies. Compared to the non-fluorinated analogs, the fluorinated porphyrins showed enhanced singlet oxygen producing efficiency.

The in-vitro photosensitizing efficacy of the fluorinated porphyrins was investigated in RIF tumors at various doses and showed promising activity. The synthesis, photophysical characteristics and in-vitro photosensitizing results of the newly synthesized fluorinated porphyin-based compounds will be discussed.

Paper to be submitted

Fluorinated Photosensitizers: Synthesis, Photophysical, Electrochemical, Intracellular Localization and *In-Vitro* Photosensitizing Efficacy

Suresh K. Pandey,[1] Amy L. Gryshuk,[1] Andrew Graham,[2] Kei Ohkubo,[3]

Shunichi Fukuzumi,[3*] Mahabeer Dobhal,[1] Gang Zheng,[1] Zhongping Ou , [4] Riqiang Zhan,[4]

Karl M. Kadish,[4*] Allan Oseroff,[2] S. Ramaprasad,[5] and Ravindra K. Pandey[1,6*]

[1]Photodynamic Therapy Center, [2]Department of Dermatology, [6]Department of Nuclear Medicine, Roswell Park Cancer Institute, Buffalo, NY 14263, USA.

[3]Department of Material and Life Sciences, Graduate School of Engineering, Osaka University, CREST, Japan Science and Technology Corporation (JST), Yamada-oka, Suita, Osaka 565-0871, Japan.

[4]Department of Chemistry, University of Houston, Houston, TX 77204-5003, USA.

[5]Department of Radiology, University of Nebraska, Omaha, Nebraska, USA

Address for correspondence:

Ravindra.pandey@roswellpark.org

Kkadish@uh.edu

Fukuzumi@ap.chem.eng.osaka-u.ac.jp

Abstract:

For *in vivo* NMR imaging, starting from pyrroles, a series of fluorinated porphyrins were synthesized by following the MacDonald reaction conditions. Fluorinated porphyrin **4** containing four trifluoromethyl groups (12 fluorine units) on reacting with osmium tetroxide was converted into the related chlorin **30** and bacteriochlorin **31** exhibiting long-wavelength absorptions at 652 and 720 nm, respectively. All these compounds produced good singlet oxygen production efficiency. The fluorinated substituents have no adverse effects on the photophysical properties of porphyrins, chlorin and bacterichlorin. All these compounds were found to be quite effective *in vitro*. In a comparative intracellular localization study with Rhodamine in RIF tumor cells, the most soluble porphyrin **4** containing two propionic acid side chains, the related chlorin **30** and bacteriochlorin **31** were found to localize in mitochondria.

Introduction:

Photodynamic Therapy (PDT) is now a well recognized modality that has been used both independently and in conjunction with other cancer treatments.[1] Combining the use of a light-sensitive drug, lasers and fiber-optic probes, PDT has emerged as one of the promising strategies in cancer treatment. In this therapy, patients are given intravenous injections of a drug that accumulates in cancer cells in much higher concentrations than in normal cells. Laser light with an appropriate wavelength delivered by fiber optics to these tumor sites produces highly reactive oxygen species (e. g. $^1O_2$) that destroy the tumor cells.[2] Therefore, for a drug to be effective, it is necessary that the compound be in high concentration in tumor cells. PDT is most beneficial when laser light is delivered at a time point when the photosensitizer's concentration is greater in the tumor than in the surrounding tissue. Thus a comprehensive knowledge of the extent of localization and the rate of accumulation is of immense value. While the photosensitizer's concentration in tissue may be determined by chemical extraction techniques, these methods are invasive, time consuming, and clinically non-feasible. In contrast, *in vivo* NMR is completely noninvasive, safe, and the therapy can be monitored over time in a single living system.[3]

In vivo MR spectroscopy has been used increasingly to monitor metabolism and disease states in humans. Both magnetic resonance imaging and spectroscopy have evolved into sophisticated diagnostic techniques. In addition to the proton, nuclei such as fluorine[4] can be studied by *in vivo* spectroscopy and imaging. Fluorine-19 (^{19}F) NMR is a technique with significant potential because of the relatively high sensitivity and low endogenous background. Due in part to its high natural abundance and high MR sensitivity, fluorine has received considerable attention as an MR nucleus. Fluorine-19 MR has been used to study metabolism, tumor growth, and blood flow.[5] More recently, *in vivo* ^{19}F MR has been used to measure tumor

integrity and vasculature in subcutaneously implanted tumors in rats[6]. MR of fluorinated compounds is particularly attractive for *in vivo* studies of human and animal models. The ^{19}F isotope has a 100% natural abundance, a spin of 1/2, and a MR sensitivity that is 83% then that of hydrogen[7].

To date, most of the fluorinated porphyrin-based analogs synthesized for *in vivo* ^{19}F NMR studies have been unsymmetrical,[8] and thus lead to signal dispersion. In order to have a strong fluorine signal at a low concentration of the drug in tumor, it is necessary to have photosensitizers containing multiple fluorine units. It would be advantageous to have a center of symmetry in the fluorinated photosensitizer that will render the fluorine nuclei to be equivalent and provide signal addition of all equivalent nuclei.

Result and Discussion:

Chemistry:

For the synthesis of porphyrin-based fluorinated photosensitizers, our synthetic strategy was divided into two parts: (a) synthesis of porphyrins **1** and **2** containing symmetrical trifluoromethyl groups (total fluorine: 6) introduced at the *meta-* or *para*-position(s) of the phenyl ring, (b) porphyrins **3** and **4** bearing symmetrical trifluoromethyl groups introduced at 3 and 5-positions (total fluorine: 12) of the phenyl ring present at the *meso*-position of the porphyrin ring system.

Porphyrins **1- 4** were synthesized from pyrroles **5**,[9] **15**[10] or **19**[11] by following the well established "2 + 2" reaction approach.[12] In brief, reactions of pyrrole **5** with *p*-, *m*- or 3', 5'-dimethoxyphenyl aldehyde under acidic reaction conditions produced the corresponding dipyrromethanes **6**, **7** and **8** in >80% yield, which on refluxing with ethylene glycol/KOH gave the related α–free dipyrromethanes **9**, **11** and **13** respectively in >85 % yield. Further reaction of

these pyrromethane with $POCl_3$/DMF under Vilsmeier's reaction conditions[13] produced the corresponding diformyl dipyrromethanes **10**, **12** and **14** in excellent yields (>75%). For the preparation of pyrromethane **17**, pyrrole **15** was first converted into the acetoxy derivative **16**, which on treating with K-10 clay[14] in dichloromethane at room temperature gave the desired dipyrromethane in 70% overall yield. Reaction of pyrrole **19** with bromine/methanol[15] gave the corresponding dipyrromethane **20** in 72% yield. Hydrogenation of pyrromethane **17** and **20** in presence of Pd/C at room temperature produced the corresponding carboxylic acids **18** and **21** in quantitative yields.

Diformyldiyrromethanes **12**, **13** and **14** were then individually reacted with dipyrromethane dicarboxylic acid **18** under McDonald reaction conditions.[12] After purification porphyrins **22-24** were isolated in 33-35% yields. By following a similar approach, pyrromethane **14** was also reacted with pyrromethane dicarboxylic acid **21**, and porphyrin **25** was obtained in 38% yield. For the preparation of fluorinated analogs, porphyrins **22-25** containing methoxy groups in the phenyl rings were reacted with boron-tribromide and the related hydroxy-phenyl porphyrins **26-29** were obtained in 68-70% yields. Further reaction of these porphyrins with 3,5-bis(trifluoromethyl)benzyl alcohol produced the desired fluorinated porphyrins **1- 4** in good yield. The structures of the intermediates and the final products were confirmed by ^1H, ^{19}F NMR, mass spectrometry and elemental analyses.

Among the fluorinated porphyrins, compound **4** containing two- propionic ester functionalities at the bottom half of the molecule showed enhanced solubility in 1% Tween 80/water formulation as well as improved *in vitro* photosensitizing efficacy than the other analogs. Therefore, for investigating the photosensitizing effect(s) of fluorinated groups in long-wavelength absorbing compounds, porphyrin **4** was reacted with osmiumtetroxide (OsO_4) and

the corresponding *vic*-dihydroxy chlorin **30** (λ_{max}: 648 nm) and tetra-hydroxy-bacteriochlorin **31** (as an isomeric mixture, λ_{max}: 716 nm) were synthesized. The yield of the individual product was found to depend on the amount of OsO_4 used.

As expected, the ^{19}F NMR spectra of all the fluorinated porphyrins **1- 4** exhibited a single peak at δ 13.0 ppm due to the presence of a center of symmetry in the molecule, whereas chlorin **30** and bacteriochlorin **31** showed two-peaks with equal intensity at 12.98 and 12.99 ppm respectively.

Photophysical Properties:

A typical fluorescence spectrum of fluorinated porphyrins in PhCN is shown in Figure 1 for the case of **3** which exhibits virtually the same fluorescence maxima at 628 and 693 nm as observed for non-fluorinated porphyrins. The absorption and fluorescence maxima of investivated porphyrins **1-4, 26-29**, chlorin **30** and bacterichlorin **31** are listed in Table 1. The absorption and fluorescence maxima are not affected by the fluorinated substituents and they are red-sifted in order: porphyrin, chlorin and bacteriochlorin.

Table 1, Figure 1

The fluorescence decay of **3** is fitted well by a single-exponential line with lifetime of 18.5 ns as shown in Figure 2. The fluorescence lifetimes were determined from the slope of the first-order plot (Figure 2) and they are also listed in Table 1. The fluorescence lifetimes (τ) are also unaffected by fluorinated substituents. The τ values of porphyrins are all similar in the range of 17.3 – 18.6 ns irrespective of substituents, but they are significantly longer than those of clorin (**30**: 3.8 ns) and bacteriochlorin (**31**: 3.3 ns).

Figure 2

Phosphorescence spectra are observed in deaerated frozen 2-MeTHF at 77 K. The phosphorescence maxima are also summarized in Table 1. Again the phosphorescence maxima of porphyrins (822-823 nm) are not affected by fluorinated subsiturents. The triplet excited states of porphyrin are detected from the transient absorption spectra measured 4.0 ns after laser excitation at 355 nm. A typical example is shown in Figure 3 for the case of **3**. The negative

Figure 3

absorption at 410 nm in Figure 3 are due to bleaching of the ground-state absorption bands. The positive absorption at 450 nm in Figure 3 are due to the triplet-triplet (T-T) transition. The T-T absorption decay obeys first-order kinetics as shown in Figure 4. This indicates that there is no

Figure 4

contribution of the triplet-triplet annihilation under the present experimental conditions. The T-T absorption maxima and the triplet lifetimes are summarized in Table 2. The triplet lifetimes of porphyrins are in the range of 8.3–25μs, which are shorter than the lifetimes of chlorin (**30**: 185 μs) and bacteriochlorin (**31**: 77 μs).

Table 2

The decay of the T-T absorption in oxygen-saturated PhCN is enhanced significantly over

what is observed in deaerated PhCN. The decay kinetics obey first-order kinetics and the decay rate constant increases with increasing oxygen concentration. Thus, an efficient energy transfer from the triplet excited state of **3** to oxygen occurs to produce singlet oxygen. The rate constants of the energy transfer (k_{EN}) were determined from the dependence of the decay rate constants on oxygen concentration as listed in Table 2. The k_{EN} values are in the range of 5.8 x 10^8 – 1.1 x 10^9 M^{-1} s^{-1}. There is no specific effects of the fluorinated substituents on the k_{EN} values which are smaller than the diffusion-limited value in PhCN (5.6 x 10^9 M^{-1} s^{-1}).[1]

Irradiation of an oxygen-saturated benzene solution of **3** results in formation of singlet oxygen which was detected by the $^1O_2$ emission at 1270 nm (see Experimental Section). Quantum yields (Φ) of $^1O_2$ generation were determined from the emission intensity which was compared to the intensity obtained using a C_{60} reference compound.[16] Relatively high Φ values are obtained for all investigated compounds as summarized in Table 2. The highest Φ value is obtained as 0.81 for the tetrafluorinated compound **3**.

Electrochemical Studies:

The fourteen investigated compounds can be divided into three groups based on the macrocycle and different substituents on the macrocycle. The first group includes five fluorinated porphyrins. The second group complex includes five non-fluorinated porphyrins and the third group includes four fluorinated or non-fluorinated chlorins and bacteriochlorin.

The electrochemistry of these three group complexes was carried out in PhCN containing 0.1 M TBAP as a supporting electrolyte. Typical cyclic voltammograms are shown in Figure 5 and the overall electrochemical data are summarized in Table 4. For group I complexes, two reversible reductions and at least two oxidations can be observed. The $E_{1/2}$ for the first reduction in PhCN ranges from -0.95 to -1.43 V and the second reduction ranges from -1.62 to -1.76 V

(Table 4). By comparison to other fluorinated porphyrins, one can see that compound FP-21 is easier to be reduced but harder to be oxidized in PhCN containing 0.1 M TBAP due to the electron-withdrawing group, $COCF_3$, which is directly bound to a *meso* position of the complex. The HOMO-LUMO gap for the group I ranges from 2.16 to 2.30 V (for FP-21, the value is 2.02 V).

Figure 5, Table -4

The UV-visible spectral changes obtained during thin-layer controlled-potential reduction and oxidation of each fluorinated porphyrin were recorded in PhCN containing 0.2 M TBAP. An example of the spectral changes is given in Figure 6 for the first reduction and oxidation of **3**. A summary of the overall spectral data for each neutral, electroreduced and oxidized complex is given in Table 5. The neutral compound of **3** has a single Soret band at 407 nm and four visible bands at 503, 535, 571 and 625 nm. Upon the first reduction, both the Soret and visible bands decrease in intensity while a new broad visible band appears at 801 nm (see Figure 6). The results are consistent with an electron transfer involving the porphyrin π-ring system and indicate the formation of a porphyrin π-anion radical. Upon the first oxidation, both the Soret band and the major visible band at 503 nm also decrease in intensity but no new bands can be observed. Similar spectral changes can be seen for other fluorinated porphyrins during the thin-layer oxidation or reduction.

Figures 6 and 7

The electrochemical and spectroelectrochemical behavior for group II complexes was similar to that of the group I complexes. Two reductions and at least two oxidations can be seen in PhCN, 0.1 M TBAP (see Table 4, Figure 5c and 5d). The oxidations are irreversible for all of

the OH substituented non-fluorinated porphyrins at scan rates up to 0.5 V/s. However, for compound **4a**, which has no OH group on the molecule, the first two oxidations are reversible at a scan rate of 0.5 V/s (see Figure 5c).

The Group III compounds include three chlorins and one bacteriochlorin. These four compounds have similar electrochemical behavior. Two reversible reductions can be seen in PhCN while at least three oxidations can be observed, the first of which is reversible in the same solvent. The HOMO-LUMO gap of these compounds ranges from 1.90 to 2.04 V which is smaller than in the case of porphyrins (see Table 4).

Spectroelectrochemical data of the chlorin and bacteriochlorin complexes are given in Table 5. An example of the spectral changes upon the first reduction and first oxidation are shown in Figure 7 for compound **30**. The Soret band at 402 nm and the visible bands at 535 and 648 nm decrease in intensity during controlled-potential electroreduction or electrooxidation for this chlorin complex. Two new bands at 501 and 735 nm appear upon the first reduction and only one new band at 694 nm appears upon the first oxidation. These results are similar to what was obtained for other chlorins[17] and indicate that a π anion radical or π cation radical forms upon reduction or oxidation.

Table 5

In vitro Photosensitizing Efficacy:

The *in vitro* photosensitizing activity of fluorinated photosensitizers **1-4** was determined in radiation induced fibrosarcoma (RIF) tumor cell lines.[18] For determining the drug dose, one of the fluorinated porphyins **4** was initially tested at two different concentrations (0.5 and 1.0 μM). The drug concentration at 1.0μM, together with a light dose at 4.0 J/cm^2, produced a significant

phototoxicity without any dark toxicity. Other photosensitizers were then evaluated under similar drug concentration. From the results summarized in Figure 8 it can be seen that all fluorinated porphyrins, chlorin and bacteriochlorin produced significant *in vitro* efficacy. However, in the porphyrin series, compounds containing bis-trifluoromethyl groups were found to be less effective than those containing tetra-trifluoromethyl groups. The *vic*-dihydroxy chlorin **30** and the related tetrahydroxy-bacteriochlorin **31** were quite effective with similar efficacy. In order to correlate the singlet oxygen efficiency with photosensitizing activity, these compounds were also evaluated for their photophysical characteristics. Though the presence and position of the fluorinated substituents in the porphyrin macrocycle produced a remarkable difference in singlet oxygen producing efficiency, no direct correlation was observed between singlet oxygen yield and *in vitro* photodynamic activity. For example, the singlet oxygen yields of porphyrins **1-3**, are quite similar (0.61-0.81) but these compounds showed a significant difference in photosensitizing activity. In contrast, among the tetra-trifluorinated analogs (**3** and **4**) in spite of a significant difference in singlet oxygen yields (0.81 and 0.36 respectively), similar photosensitizing results were obtained.

Figure 8

On the basis of *in vitro* results, it is difficult to predict the *in vivo* photosensitizing efficacy of these photosensitizers because the pharmacokinetic and pharmacodynamic profiles as well as photobleaching characteristics play important roles in drug localization and clearance. These properties could also be influenced by the overall lipophilicity of the molecule, which has proven to be an important molecular descriptor that often is well correlated with the bioactivity of drugs. Lipophilicity is indicated by lipophilic indices, such as logarithm of a partition coefficient, log P, which reflects the equilibrium partitioning of a molecule between a nonpolar

and a polar phase, such as n-octanol/water system. Partition coefficient can be measured either experimentally by following simple "shake flask" approach or by using currently available computer program (Pallas system). We calculated the log P values of fluorinated porphyrins **1- 4,** chlorin **30** and bacteriochlorin **31** and these were in the range of 15.58 -19.75 [**1** and **2**: 5.58, **3**: 19.75 and **4**: 18.43]. For investigating a correlation between singlet oxygen yields and PDT efficacy, the *in vivo* studies of fluorinated photosensitizers at different drug/light doses are currently in progress. These results along with the *in vivo* F-19 tumor imaging data will be reported elsewhere.

Intracellular Localization:

In general, porphyrin-based compounds have shown very diverse patterns of localization, based on structure, lipophilicity, and charge.[19] The lysosomes and the mitochondria are reported to be predominant. However, in a QSAR study of certain photosensitizer the compounds that localize in mitochondria are generally found to be more effective.[20] Therefore, the site of localization of fluorinated porphyrin **4** and the related chlorin **30** and bacteriochlorin **31** was compared with Rhodamine-123 known to target mitochondria. Images of photosensitizers and Rhodamine -123 were taken in rapid succession. The images results clearly indicated that these photosensitizers localize to the same cellular region as Rhodamine-123, suggesting that these compounds localize in mitochondria (see Figure 9, a representative example), a more sensitive site for cell damage by PDT.

Figure 9

Experimental:

Chemistry:

All chemicals were of reagent grade and used as such. Solvents were dried using standard

methods unless stated otherwise. Reactions were carried out under N_2 atmosphere and were monitored by precoated (0.20mm) silica TLC plastic sheet strips (POLYGRAM® SIL N-HR). Melting points were determined on electrically heated melting point apparatus and are uncorrected. UV-vis spectra were recorded on a Varian (Cary -50 Bio) spectrophotometer. ^1H and ^{19}F-NMR spectra were recorded on a Brucker AMX 400 and 376.5 MHz NMR spectrometer respectively at 303 K in $CDCl_3$ containing tetramethylsilane (TMS) as an internal standard. Proton chemical shifts (δ) are reported in parts per million (ppm) relative to TMS (0.00 ppm) or $CDCl_3$ (7.26 ppm) while fluorine chemical shifts are reported in ppm relative to trifluoroacetic acid (0.00 ppm). Coupling constants (J) are reported in Hertz (Hz) and s, ss, d, t, q, m and br refer to singlet, split singlet, doublet, triplet, quartet, multiplet and broad respectively. Mass spectral data were obtained from University of Michigan, East Lansing, MI and from Biopolymer Facility of Basic Studies Center, Roswell Park Cancer Institute. Elemental analysis data were obtained from Midwest Microlab, LLC, Indianapolis, IN.

General method for the synthesis of Pyrromethane 6, 7 and 8:

Pyrrole **5** (10.0g, 0.055mol) and *p*-methoxy benzaldehyde (3.74g, 0.0275mol) were dissolved in ethanol (70ml) and *p*-toluenesulfonic acid (200 mg) was added. The reaction mixture was refluxed for 2 hours under nitrogen. Analytical TLC in frequent intervals was used to monitor the completion of the reaction. It was then cooled, the solid was filtered, the product was washed with cold water and dried under vacuum at room temperature. The desired pyrromethane **6** [3,9-diethyl-6-(*p*-methoxyphenyl)-4,8-dimethyl-2,10-diethoxycarbonyl dipyrro-methane] was isolated as a white powder 21.2 g (80%).

3,9-diethyl-6-(*p*-methoxyphenyl)-4,8-dimethyl-2,10-diethoxycarbonyl dipyrromethane (6):

Mp 105-108 °C; ^1H NMR ($CDCl_3$, 400 MHz) δ 8.20(brs, 2H, 2 x NH), 7.01 (d, J = 8.9, 2H,

ArH), 6.87 (d, J = 8.9, 2H, ArH), 5.43(s, 1H, CH), 4.26 (q, J = 7.7, 14.0, 4H, 2 x $OC\underline{H}_2CH_3$), 3.81 (s, 3H, OCH_3), 2.74(q, J = 7.5, 4H, 2 x $C\underline{H}_2CH_3$), 1.78 (s, 6H, 2 x CH_3), 1.31 (t, J = 7.1, 6H, 2 x $OCH_2C\underline{H}_3$), 1.12 (t, J = 7.7, 6H, 2 x $CH_2C\underline{H}_3$). Anal. Calcd for $C_{28}H_{36}N_2O_4$: C, 69.98; H, 7.55; N, 5.83. Found: C, 70.15; H, 7.37; N, 5.93.

By following a similar approach, pyrrole **5** was reacted with *m*-methoxy or 3, 5-dimethoxy benzaldehyde and the corresponding dipyrromethane **7** and **8** were synthesized.

3,9-Diethyl-6-(*m*-methoxyphenyl)-4,8-dimethyl-2,10-diethoxycarbonyl dipyrromethane (7): Yield 70%; mp 122-125°C ; ^{1}H NMR ($CDCl_3$, 400 MHz) δ 8.25 (brs, 2H, 2 x NH), 7.23-7.27 (m, 1H, ArH), 6.82 (dd, J = 2.2, 7.8, 1H, ArH), 6.68 (d, J = 7.4, 1H, ArH), 6.63 (ss, 1H, ArH), 5.45 (s, 1H, CH), 4.25 (q, J = 7.9, 4H, 2 x $OC\underline{H}_2CH_3$), 3.76 (s, 3H, OCH_3), 2.73 (q, J = 7.6, 4H, 2 x $C\underline{H}_2CH_3$), 1.79 (s, 6H, 2 x CH_3), 1.30 (t, J = 7.1, 6H, 2 x $OCH_2C\underline{H}_3$), 1.11 (t, J = 7.3, 6H, 2 x $CH_2C\underline{H}_3$).Anal. Calcd for $C_{28}H_{36}N_2O_5$: C, 69.98; H, 7.55; N, 5.83. Found: C, 70.08; H, 7.60; N, 5.82.

3,9-Diethyl-6-(3'5'-dimethoxyphenyl)4,8-dimethyl-2,10-diethoxycarbonyldipyrromethane (8). Yield 50%; viscous oil; ^{1}H NMR ($CDCl_3$, 400 MHz) δ 8.25 (brs, 2H, 2 x NH), 6.38 (s, 1H, ArH), 6.24 (s, 2H, ArH), 5.39 (s, 1H, CH), 4.26 (q, J = 6.2, 4H, 2 x $OC\underline{H}_2CH_3$), 3.74 (s, 6H, 2 x OCH_3), 2.70 – 2.78 (m, 4H, 2 x $C\underline{H}_2CH_3$), 1.79 (s, 6H, 2 x CH_3), 1.32 (t, J = 7.2, 6H, 2 x $OCH_2C\underline{H}_3$), 1.10 – 1.16 (m, 6H, 2 x $CH_2C\underline{H}_3$).

General method for the preparation of pyrromethanes 9, 11, 13:

The foregoing diethoxycarbonyl dipyrromethanes **6**, **7** or **8** (for example 11.6g of **6**) were individually dissolved in ethylene glycol (250 ml). Sodium hydroxide (12 g, crushed powder) was added, and the reaction mixture was refluxed for 1 h. It was then cooled, diluted with dichloromethane (250 ml), and washed with water (2 x 200 ml). The dichloromethane layer

was dried over anhydrous sodium sulfate. The residue obtained after evaporating the solvent was chromatographed over silica column eluted with chloroform. The appropriate eluates were combined, the solvent was evaporated, and the desired dipyrromethane **9** was obtained in 95 % (7.70 g) yield.

3,9-diethyl-6-(p-methoxyphenyl)4,8-dimethyl-dipyrromethane (9):

Mp 64-66°C ; lit[20] ^{1}H NMR ($CDCl_3$, 400 MHz) δ 7.30 (brs, 2H, 2 x NH), 7.06 (d, J = 8.8, 2H, ArH), 6.85 (d, J = 8.8, 2H, ArH), 6.38 (ss, 2H, 2 x Pyrrolic CH), 5.45(s, 1H, CH), 3.81(s, 3H, OCH_3), 2.44 (q, J = 7.2, 4H, 2 x $C\underline{H}_2CH_3$), 1.81 (s, 6H, 2 x CH_3), 1.19 (t, J = 7.9, 6H, 2 x $CH_2C\underline{H}_3$).

3,9-Diethyl-6-(*m*-methoxyphenyl)-4,8-dimethyl-dipyrromethane (11):

Yield 88 %; mp 202-204°C; ^{1}H NMR ($CDCl_3$, 400 MHz) δ 9.49 (s, 2H, 2 x CHO), 9.08 (brs, 2H, 2 x NH), 7.23-7.27 (m, 1H, ArH), 6.83 (dd, J = 2.5, 8.0, 1H, ArH), 6.66 (d, J = 7.6, 1H, ArH), 6.62 (s, 1H, ArH), 5.53 (s, 1H, CH), 3.75 (s, 3H, OCH_3), 2.71 (q, J = 7.6, 4H, 2 x $C\underline{H}_2CH_3$), 1.86 (s, 6H, 2 x CH_3), 1.20 (t, J = 7.8, 6H, 2 x $CH_2C\underline{H}_3$). Anal. Calcd for $C_{22}H_{28}N_2O.2H_2O$: C, 70.94; H, 8.66; N, 7.52. Found: C, 69.29; H, 7.17; N, 7.24.

3, 9-Diethyl-6-(3',5'-di-methoxyphenyl)-4,8-dimethyl-dipyrromethane (13):

Yield 97 %; mp 119-121°C ; ^{1}H NMR ($CDCl_3$, 400 MHz) δ 7.34(brs, 2H, 2 x NH), 6.33 -6.36 (m, 3H, ArH), 6.31(ss, 2H, 2 x Pyrrolic CH), 5.40 (ss, 1H, CH), 3.74(s, 6H, 2 x OCH_3), 2.40 – 2.45 (m, 4H, 2 x $C\underline{H}_2CH_3$), 1.81(s, 6H, 2 x CH_3), 1.14 – 1.19 (m, 6H, 2 x $CH_2C\underline{H}_3$). Anal. Calcd for $C_{23}H_{30}N_2O_2.5H_2O$: C, 60.50; H, 8.83; N, 6.40. Found: C, 60.00; H, 6.82; N, 5.91.

General method for the preparation of diformyldipyrromethanes 10, 12 and 14:

The foregoing pyrromethane(s) [e. g. **9** (7.1g)] was dissolved in Vilsmeier reagent, prepared by reaction $POCl_3$ (10.5 ml) and DMF (45 ml) was added and the reaction mixture was stirred at

room temperature overnight. The reaction mixture was poured in ice cold water (250 ml) and aqueous sodium hydroxide (50%, 35 ml) was then added slowly and the pH was adjusted 10-12 , and stirred overnight before extracting with dichloromethane (3 x 200 ml). The organic layer was separated, washed with water (2 x 200 ml) until neutral and dried over anhydrous sodium sulfate. Evaporation of the solvent gave a residue which was chromatographed over a silica column, eluting with 1 : 1 ethyl acetate/ cyclohexane. The major band was separated, and the product obtained after evaporating the solvent was crystallized with methanol and compound **10** was isolated in 80%(6.80g) yield.

3,9-Diethyl- 2,10-diformyl-6-(*p*-methoxyphenyl)-4,8-dimethyl-dipyrromethane (10):

Mp 168-169°C; ^{1}H NMR ($CDCl_3$, 400 MHz) δ 9.50 (s, 2H, 2 x CHO), 8.70 (brs, 2H, 2 x NH), 6.98(d, J = 8.7, 2H, ArH), 6.86 (d, J = 8.7, 2H, ArH), 5.47 (s, 1H, CH), 3.80(s, 3H, OCH_3), 2.70(q, J = 7.5, 4H, 2 x $C\underline{H}_2CH_3$), 1.81 (s, 6H, 2 x CH_3), 1.20 (t, J = 7.5, 6H, 2 x $CH_2C\underline{H}_3$). Anal. Calcd for $C_{24}H_{28}N_2O_3.1/2\ H_2O$: C, 71.80; H, 7.28; N, 6.98. Found: C, 71.69; H, 6.74; N, 6.76.

3,9-Diethyl-2,10-diformyl-6-(*m*-methoxyphenyl)-4,8-dimethyl-dipyrromethane (12):

Yield 79 %; mp 202-204°C; ^{1}H NMR ($CDCl_3$, 400 MHz) δ 9.49 (s, 2H, 2 x CHO), 9.08 (brs, 2H, 2 x NH), 7.23-7.27(m, 1H, ArH), 6.83 (dd, J = 2.5, 8.0, 1H, ArH), 6.66 (d, J = 7.6, 1H, ArH), 6.62(s, 1H, ArH), 5.53(s, 1H, CH), 3.75 (s, 3H, OCH_3), 2.71 (q, J = 7.6, 4H, 2 x $C\underline{H}_2CH_3$), 1.86(s, 6H, 2 x CH_3), 1.20 (t, J = 7.8, 6H, 2 x $CH_2C\underline{H}_3$). Anal. Calcd for $C_{24}H_{28}N_2O_3$: C, 73.44; H, 7.19; N, 7.14. Found: C, 73.65; H, 7.29; N, 7.06.

3,9-Diethyl-2,10-diformyl-6-(3,5-di-methoxyphenyl)-4,8-dimethyl-dipyrromethane 14:

Yield 78 %; mp 202-204°C; ^{1}H NMR ($CDCl_3$, 400 MHz) δ 9.52 (s, 2H, 2 x CHO), 8.56(brs, 2H, 2 x NH), 6.40 (s, 1H, ArH), 6.20 (ss, 2H, ArH), 5.42 (s, 1H, CH), 3.74 (s, 6H, 2 x OCH_3), 2.70(q, J = 7.7, 4H, 2 x $C\underline{H}_2CH_3$), 1.81 (s, 6H, 2 x CH_3), 1.20 (t, J = 7.8, 6H, 2 x $CH_2C\underline{H}_3$). Anal. Calcd

for $C_{25}H_{30}N_2O_4.1/2H_2O$: C, 69.58; H, 7.24; N, 6.49. Found: 69.52; H, 7.00; N, 6.16.

General method for the Synthesis of porphyrins 22-25:

The diformyl dipyrromethane (e. g. **10**, 2.52g, 6.43 mmol), and dipyrromethane **18**(2.04g, 6.42 mmol) were dissolved in dichloromethane (500 ml). *p*-Toluenesulfonic acid (6.0g) dissolved in methanol (100ml) was added, and the reaction mixture was stirred at room temperature overnight under nitrogen atmosphere. A saturated solution of zinc acetate/methanol (125ml) was added, and the reaction was stirred for another 12 hours. It was then diluted with dichloromethane, washed with water, and the organic layer was dried over anhydrous sodium sulfate. Evaporation of the solvent gave a residue, which was dissolved in trifluoroacetic acid (30ml) and stirred at room temperature for 30 min. The Zn-free porphyrin thus obtained after the standard work-up was chromatographed over a short Grade III Alumina column, eluted with dichloromethane. The major band was collected, and the solvent evaporated. The residue was crystallized from dichloromethane/hexane and porphyrin **22** was isolated in 17% (640 mg) yield.

2, 8, 13, 17-Tetraethyl-5-(*p*-methoxyphenyl)-3,7,12,18-tetramethylporphyrin (22):

Mp 280-282°C; UV-vis (CH_2Cl_2) 403(3.82×10^5), 503(3.15×10^4), 535(1.39×10^4), 571(1.35×10^4), 623(4.82×10^3); ^{1}H NMR ($CDCl_3$, 400 MHz) δ 10.13(s, 2H, 2 x mesoH), 9.92(s, 1H, mesoH), 7.86(d, J = 9.0, 2H, ArH), 7.16(d, J = 9.0, 2H, ArH), 4.00 – 4.06(m, 8H, 4 x $C\underline{H}_2CH_3$), 3.99 (s, 3H, OCH_3), 3.62(s, 6H, 2 x CH_3), 2.47(s, 6H, 2 x CH_3), 1.87(t, J = 7.7, 6H, 2 x $CH_2C\underline{H}_3$), 1.75(t, J = 7.6, 6H, 2 x $CH_2C\underline{H}_3$), -3.19(brs, 1H, NH), -3.27(brs, 1H, NH), Anal. Calcd for $C_{39}H_{44}N_4O$: C, 80.10; H, 7.58; N, 9.58. Found: C, 80.14; H, 7.54; N, 9.62.

2, 8, 13, 17-Tetraethyl-5-(*m*-methoxyphenyl)-3,7,12,18-tetramethylporphyrin (23):

Yield 30%; mp 270-272°C; ^{1}H NMR ($CDCl_3$, 400 MHz) δ10.16(s, 2H, 2 x mesoH), 9.96(s, 1H, mesoH), 7.67(d, J = 7.2, 2H, ArH), 7.59(t, J = 7.8, 1H, ArH), 7.50(s, 1H, ArH), 4.02 – 4.10(m,

8H, 4 x $C\underline{H}_2CH_3$), 4.00 (s, 3H, OCH_3), 3.65(s, 6H, 2 x CH_3), 2.60(s, 6H, 2 x CH_3), 1.90(t, J = 7.7, 6H, 2 x $CH_2C\underline{H}_3$), 1.78(t, J = 7.94, 6H, 2 x $CH_2C\underline{H}_3$), -3.20(brs, 1H, NH), -3.35(brs, 1H, NH). Anal. Calcd for $C_{39}H_{44}N_4O$: C, 80.10; H, 7.58; N, 9.58; Found: C, 80.76; H, 7.60; N, 9.54.

2, 8-Diethyl-5-(3',5'-di-methoxyphenyl)-2, 8-diethyl- 13, 17- bis- (2-methoxycarbonylethyl)-3, 7, 12, 18-tetramethylporphyrin (25):

The title compound was prepared by reacting diformyldipyrromethane **14** with pyrromethane dicarboxylic acid **21** by following the procedure reported by Chen et al [Ref].

General method for the synthesis of porphyrins 26-29:

Porphyrin **26-29** were obtained in 70-77% by reacting porphyrins **22-25** with etherial boron tribromide solution.

2, 8, 13, 17-tetraethyl-5-(*p*-hydroxyphenyl)-3,7,12,18-tetramethylporphyrin (26):

Yield --; mp > 300°C; UV-vis (CH_2Cl_2) 404(3.79×10^5), 503(2.91×10^4), 536(1.19×10^4), 570(1.14×10^4); ^{1}H NMR ($CDCl_3$, 400 MHz) δ 10.15 (s, 2H, 2 x mesoH), 9.94 (s, 1H, mesoH), 7.89(d, J = 9.2, 2H, ArH), 7.18 (d, J = 8.7, 2H, ArH), 4.00 – 4.08 (m, 8H, 4 x $C\underline{H}_2CH_3$), 3.64 (s, 6H, 2 x CH_3), 2.53 (s, 6H, 2 x CH_3), 1.88 (t, J = 7.7, 6H, 2 x $CH_2C\underline{H}_3$), 1.76 (t, J = 7.5, 6H, 2 x $CH_2C\underline{H}_3$), -3.85 - -3.75(brs, 2H, 2 x NH). Anal. Calcd for $C_{38}H_{42}N_4O$: C, 79.66; H, 7.42; N, 9.82; Found: C, 79.75; H, 7.45; N, 9.70.

2, 8, 13, 17-tetraethyl-5-(*m*-hydroxyphenyl)-3,7,12,18-tetramethylporphyrin (27):

Yield --%; mp > 300°C; UV-vis (CH_2Cl_2) 402(5.00×10^5), 502(4.03×10^4), 536(1.76×10^4), 570(1.61×10^4), 623 (4.60×10^3); ^{1}H NMR ($CDCl_3$, 400 MHz) δ 10.18 (s, 2H, 2 x mesoH), 9.98 (s, 1H, mesoH), 7.69 (d, J = 7.0, 2H, ArH), 7.61(t, J = 7.7, 1H, ArH), 7.51(s, 1H, ArH), 4.04 – 4.12(m, 8H, 4 x $C\underline{H}_2CH_3$), 3.66(s, 6H, 2 x CH_3), 2.58 (s, 6H, 2 x CH_3), 1.91 (t, J = 7.7, 6H, 2 x $CH_2C\underline{H}_3$), 1.79 (t, J = 7.94, 6H, 2 x $CH_2C\underline{H}_3$), -3.85 - -3.75(brs, 2H, 2 x NH); Anal. Calcd for

$C_{38}H_{42}N_4O$: C, 79.66; H, 7.42; N, 9.82. Found: C, 80.02; H, 7.37; N, 9.83.

2, 8, 13, 17-tetraethyl-5-(3',5'-di-hydroxyphenyl)-3,7,12,18-tetramethylporphyrin (28):

Yield --%; mp > 300°C ; UV-vis (CH_2Cl_2) 402 (4.16 x 10^5), 502 (3.45 x 10^4), 536 (1.62 x 10^4), 569 (1.49 x 10^4), 623 (6.50 x 10^3); ^{1}H NMR ($CDCl_3$, 400 MHz) δ 10.18 (s, 2H, 2 x mesoH), 9.98 (s, 1H, mesoH), 7.05 (s, 2H, ArH), 6.69 (s, 1H, ArH), 4.04 – 4.12 (m, 8H, 4 x $C\underline{H}_2CH_3$), 3.66 (s, 6H, 2 x CH_3), 2.67 (s, 6H, 2 x CH_3), 1.90 (t, J = 7.7, 6H, 2 x $CH_2C\underline{H}_3$), 1.80 (t, J = 7.5, 6H, 2 x $CH_2C\underline{H}_3$). Anal. Calcd for $C_{38}H_{42}N_4O_2.H_2O$: C, 75.47; H, 7.33; N, 9.26. Found: C, 75.31; H, 7.38; N, 9.14.

2, 8-Diethyl-5-(3',5'-di-methoxyphenyl)- 13, 17- bis-(2-methoxycarbonylethyl)-3, 7, 12, 18-tetramethylporphyrin (29):

Yield --%; mp > 300°C; UV-vis (CH_2Cl_2) 403(4.64 x 10^5), 502(5.21 x 10^4), 536(3.39 x 10^4), 571(4.00 x 10^4); ^{1}H NMR ($CDCl_3$, 400 MHz) δ 10.18(s, 2H, 2 x mesoH), 9.95(s, 1H, mesoH), 7.10(s, 2H, ArH), 6.70(s, 1H, ArH), 4.30 – 4.40(m, 4H, 2 x $C\underline{H}_2CH_2CO_2CH_3$), 3.98 – 4.08(m, 4H, 2 x $C\underline{H}_2CH_3$), 3.70(s, 6H, 2 x OCH_3), 3.65(s, 6H, 2 x CH_3), 3.30 – 3.40(m, 4H, 2 x $CH_2C\underline{H}_2CO_2CH_3$), 2.66(s, 6H, 2 x CH_3), 1.80 - 1.90(m, 6H, 2 x $CH_2C\underline{H}_3$). Anal. Calcd for $C_{42}H_{46}N_4O_6.H_2O.1/2Na_2SO_4$: C, 63.69; H, 6.11; N, 7.08. Found: C, 62.32; H, 6.07; N, 6.41.

General method for the synthesis of porphyrins 1 to 4:

3,5-bis(trifluromethyl)benzylbromide (40μL, 0.22mmol) and anhydrous K_2CO_3 (250mg) were added to a stirred solution of 5-(4-hydoxyphenyl)tetraethylporphyrin **26** (85mg, 0.15mmol) in dry acetonitrile (10 ml) and the reaction mixture was refluxed overnight under nitrogen. Solvent was evaporated under reduced pressure; water (20 ml) was poured and extracted with CH_2Cl_2 (2x 20 ml). The combined organic extracts were washed with water (2x 20 ml) and organic fraction was dried over Na_2SO_4. Removal of organic solvent *in vacuo* gave a crude solid

residue, which was chromatographed over silica column using CH_2Cl_2 as an eluant to yield 77mg (65%) of 5-[4-{3,5-bis(trifluromethyl)benzyloxy}phenyl]tetraethylporphyrin **1** as purple plates.

5-[4-{3,5-Bis(trifluromethyl)benzyloxy}phenyl]-2,8,13,17-tetraethyl-3,7,12,18-tetramethyl porphyrin (1):

Mp 274-276°C; UV-vis (CH_2Cl_2) 403(2.52 x 10^5), 502(2.08 x 10^4), 535(9.25 x 10^3), 570(8.82 x 10^3), 624(3.13 x 10^3); ^{1}H NMR ($CDCl_3$, 400 MHz) δ 10.21 (s, 2H, 2x meso C<u>H</u>), 10.00 (s, 1H, meso C<u>H</u>), 8.14 (s, 2H, Ar<u>H</u>), 7.98 (s, 1H, Ar<u>H</u>), 7.96 (d, J=4.5, 2H, Ar<u>H</u>), 7.31 (d, J=4.5, 2H, Ar<u>H</u>), 5.42 (s, 2H, OC<u>H</u>$_2$), 4.06-4.13 (m, 8H, 4x C<u>H</u>$_2$CH$_3$), 3.70 (s, 6H, 2x C<u>H</u>$_3$), 2.52 (s, 6H, 2x C<u>H</u>$_3$), 1.94 (t, J=7.7, 6H, 2x CH$_2$C<u>H</u>$_3$), 1.82 (t, J=7.5, 6H, 2x CH$_2$C<u>H</u>$_3$). ^{19}F NMR ($CDCl_3$, 376.5 MHz): δ 13.12 (s, 6F, 2 x CF_3). Anal. Calcd for $C_{47}H_{46}N_4F_6O.H_2O$: C, 69.27; H, 5.94; N, 6.87; F 13.99. Found: C, 70.37; H, 6.19; N, 6.33; F 12.89.

5-[3-{3,5-Bis(trifluromethyl)benzyloxy}phenyl]-2,8,13,17-tetraetyhl-3,7,12,18-tetramethyl porphyrin (2) :

Yield 96%; mp 109-11°C; UV-vis (CH_2Cl_2) 404(9.49 x 10^4), 501(6.83 x 10^3), 537(4.27 x 10^3), 570(4.98 x 10^3); ^{1}H NMR ($CDCl_3$, 400 MHz) δ 10.17 (s, 2H, 2x meso C<u>H</u>), 9.96 (s, 1H, meso C<u>H</u>), 7.94 (s, 2H, Ar<u>H</u>), 7.75-7.85 (m, 3H, Ar<u>H</u>), 7.62 (t, J=7.8, 1H, Ar<u>H</u>), 7.40 (dd, J=2.6 & 7.8, 1H, Ar<u>H</u>), 5.32 (s, 2H, OC<u>H</u>$_2$), 4.00-4.10 (m, 8H, 4x C<u>H</u>$_2$CH$_3$), 3.65 (s, 6H, 2x C<u>H</u>$_3$), 2.53 (s, 6H, 2x C<u>H</u>$_3$), 1.89 (t, J=7.8, 6H, 2x CH$_2$C<u>H</u>$_3$), 1.77 (t, J=7.6, 6H, 2x CH$_2$C<u>H</u>$_3$), -3.10- -3.30 (brs, 2H, 2 x NH).^{19}F NMR ($CDCl_3$, 376.5 MHz): δ 13.00 (s, 6F, 2 x CF_3). Anal. Calcd for $C_{47}H_{46}N_4F_6O.Na_2SO_4$: C, 60.12; H, 4.94; N, 5.96. Found: C 62.40, H 4.85, N 5.26.

5-[3,5-Bis{3,5-bis(trifluromethyl)benzyloxy}phenyl]-2,8,13,17-tetraethyl-3,7,12,18-tetra-methyl porphyrin (3):

Yield 45%; mp 214-216°C; UV-vis (CH_2Cl_2) 403(2.29 x 10^5), 502(1.93 x 10^4), 536(9.27 x 10^3),

570(8.53 x 10^3), 623(3.34 x 10^3); ^{1}H NMR ($CDCl_3$, 400 MHz): δ 10.20 (s, 2H, 2x meso C<u>H</u>), 9.98 (s, 1H, meso C<u>H</u>), 7.96 (s, 4H, Ar<u>H</u>), 7.87 (s, 2H, Ar<u>H</u>), 7.42 (d, J=2.9, 2H, Ar<u>H</u>), 7.12-7.16 (m, 1H, Ar<u>H</u>), 5.37 (s, 4H, 2 x OC<u>H</u>$_2$), 4.03-4.10 (m, 8H, 4x C<u>H</u>$_2$CH$_3$), 3.66 (s, 6H, 2x C<u>H</u>$_3$), 2.60 (s, 6H, 2x C<u>H</u>$_3$), 1.91 (t, J=7.5, 6H, 2x CH$_2$C<u>H</u>$_3$), 1.78 (t, J=7.5, 6H, 2x CH$_2$C<u>H</u>$_3$). ^{19}F NMR ($CDCl_3$, 376.5 MHz) δ 12.98 (s, 12F, 4 x CF_3). Anal. Calcd for $C_{56}H_{50}N_4F_{12}O_2$: C, 64.74; H, 4.85; N, 5.39. Found: C, 63.20; H, 4.94; N, 5.00.

5-[3,5-Bis{3,5-bis(trifluromethyl)benzyloxy}phenyl]-2,8-diethyl-13,17-bis(2-methoxycarbonylethyl)porphyrin (4) :

Yield 75%; mp 72-75°C; UV-vis (CH_2Cl_2) 404(3.81 x 10^5), 502(3.02 x 10^4), 536(1.41 x 10^4), 570(1.32 x 10^4), 624(4.82 x 10^3), 653(2.59 x 10^3); ^{1}H NMR ($CDCl_3$, 400 MHz) δ 10.16 (s, 2H, 2x meso C<u>H</u>), 9.97 (s, 1H, meso C<u>H</u>), 7.92 (s, 3H, Ar<u>H</u>), 7.81-7.84 (m, 3H, Ar<u>H</u>), 7.37 (d, J=2.0, 2H, Ar<u>H</u>), 7.11 (d, J=2.4, 1H, Ar<u>H</u>), 5.35 (s, 4H, 2 x OC<u>H</u>$_2$), 4.40 (t, J=7.6, 4H, 2x C<u>H</u>$_2$CH$_2$CO$_2$CH$_3$), 4.00 (q, J=7.8, 4H, 2x C<u>H</u>$_2$CH$_3$), 3.67 (s, 6H, 2 x OCH$_3$), 3.66 (s, 6H, 2x C<u>H</u>$_3$), 3.30 (t, J=7.6, 4H, 2x CH$_2$C<u>H</u>$_2$CO$_2$CH$_3$), 2.56 (s, 6H, 2x C<u>H</u>$_3$), 1.74 (t, J=7.4, 6H, 2x CH$_2$C<u>H</u>$_3$), -3.27 (brs, 1H, NH), -3.33 (brs, 1H, NH). ^{19}F NMR ($CDCl_3$, 376.5MHz) δ 12.96 (s, 12F, 4 x CF_3). Anal. Calcd for $C_{60}H_{54}N_4F_{12}O_6$: C, 62.39; H, 4.71; N, 4.85; F, 19.74. Found: C, 61.56; H, 4.71; N, 4.71; F, 19.36.

5-{3,5-Bis(3,5-dimethylbenzyloxy)phenyl}diethyldimethoxypropionateporphyrin (4a):

Yield 30%; mp 158-160°C; UV-vis (CH_2Cl_2) 404(3.81 x 10^5), 502(3.43 x 10^4), 536(1.56 x 10^4), 570(1.50 x 10^4), 623(5.19 x 10^3); ^{1}H NMR ($CDCl_3$, 400 MHz) δ 10.18 (s, 2H, 2x meso C<u>H</u>), 9.98 (s, 1H, meso C<u>H</u>), 7.31-7.32 (m, 2H, ArH), 7.11 (brs, 1H, Ar<u>H</u>), 7.08 (s, 3H, Ar<u>H</u>), 6.99 (s, 1H, Ar<u>H</u>), 6.96 (brs, 2H, Ar<u>H</u>), 5.17 (s, 4H, 2 x OC<u>H</u>$_2$), 4.42 (t, J=7.6, 4H, 2x C<u>H</u>$_2$CH$_2$CO$_2$CH$_3$), 4.04 (q, J=7.0, 4H, 2x C<u>H</u>$_2$CH$_3$), 3.70 (s, 6H, 2 x OCH$_3$), 3.69 (s, 6H, 2x C<u>H</u>$_3$), 3.32 (t, J=7.8,

4H, 2x $CH_2C\underline{H}_2CO_2CH_3$), 2.58 (s, 6H, 2x $C\underline{H}_3$), 2.30 (s, 12H, 4x $PhC\underline{H}_3$), 1.78 (t, J=7.4, 6H, 2x $CH_2C\underline{H}_3$), -3.25 (brs, 1H, NH), -3.28 (brs, 1H, NH). Mass Calcd for $C_{60}H_{66}N_4O_6$: 939.22. Found: 939.20

Synthesis of chlorin 30 and bacteriochlorin 31 from porphyrin 4:

75 mg of OsO_4 dissolved in diethyl ether (5 ml) was added to a stirred solution of **4** in dry CH_2Cl_2 (20 ml) and pyridine (0.2 ml) at room temperature, septum was applied and stirred for 6 hrs. UV-vis showed two peaks at bathochromic region viz. at 645 (chlorin, major, $R_f = 0.6$ in 5% MeOH in CH_2Cl_2) **30** and at 713 (bacteriochlorin, minor, $R_f = 0.4$ in 5% MeOH in CH_2Cl_2) **31**. Worked up the reaction by passing a stream of H_2S gas for one minute, diluted with CH_2Cl_2 (50 ml) and then filtered through fluted filter paper. Washed the residue with CH_2Cl_2 (3 x 50 ml), dried over Na_2SO_4. The solvent was concentrated and the crude mixture obtained was purified by preparative TLC using 5% MeOH in CH_2Cl_2 as eluant. Three bands were isolated. The fast moving band (10 mg) was identified as unreacted starting material **4**, middle band (25 mg, 40%) was found to be chlorin **30** and the lowest moving band isolated in 13 mg (20%) was characterized as bacteriochlorin **31**.

5-[3,5-bis{3,5-bis(trifluromethyl)benzyloxy}phenyl]-2,8-diethyl-7,8-dihydroxy-3,7,12,18-tetramethyl-13,17-bis(2-methoxycarbonylethyl)porphyrin (30):

Mp 172-174°C; UV-vis (CH_2Cl_2) 397 (4.44×10^5), 500 (4.16×10^4), 648(1.17×10^5); ^1H NMR ($CDCl_3$, 400 MHz) δ 9.88 (s, 1H, meso C$\underline{H}$), 9.61 (s, 1H, meso C$\underline{H}$), 9.21 (s, 1H, meso C$\underline{H}$), 7.97 (s, 2H, ArH), 7.91 (s, 2H, ArH), 7.88 (s, 1H, ArH), 7.84 (s, 1H, Ar$\underline{H}$), 7.35 (s, 1H, Ar$\underline{H}$), 7.12 (s, 1H, Ar$\underline{H}$), 7.06 (s, 1H, Ar$\underline{H}$), 5.40 (s, 2H, $OC\underline{H}_2$), 5.30 (s, 2H, $OC\underline{H}_2$), 4.24 (t, J=7.2, 2H, $C\underline{H}_2CH_2CO_2CH_3$), 4.15 (t, J=7.4, 2H, $C\underline{H}_2CH_2CO_2CH_3$), 3.96 (q, J=7.4, 2H, $C\underline{H}_2CH_3$), 3.69 (s, 3H, OCH_3), 3.67 (s, 3H, $OC\underline{H}_3$), 3.47 (s, 3H, $C\underline{H}_3$), 3.44 (s, 3H, $C\underline{H}_3$), 3.17 (t, J=7.6, 4H, 2x

$CH_2\underline{CH_2}CO_2CH_3$), 2.26 (s, 3H, $C\underline{H_3}$), 2.23-2.34 (m, 3H, $C\underline{H_3}$), 1.70 (t, J=7.8, 3H, $C\underline{H_3}$), 0.89-0.93 (m, 2H, $C\underline{H_2}CH_3$), 0.44 (t, J=8.0, 3H, $CH_2C\underline{H_3}$), -2.32 (brs, 1H, NH), ^{19}F NMR ($CDCl_3$, 376.5 MHz): δ 12.98 (s, 6F, 2 x CF_3), 12.99 (s, 6F, 2 x CF_3). Mass Calcd. for $C_{60}H_{56}N_4F_{12}O_8$: 1189.12. Found: 1189.50

5-[3,5-bis{3,5-bis(trifluromethyl)benzyloxy}phenyl]-2,8-diethyl-7,8,17,18-tetrahydroxy-3,7,12,18-tetramethyl-13,17-bis (2-methoxycarbonylethyl)porphyrin (31).

Mp 100-103°C; UV-vis (CH_2Cl_2) 395(1.69 x 10^5), 504(2.22 x 10^4), 644(3.81 x 10^4), 716 (2.67 x 10^4). Note : Due to mixture of isomers it was difficult to assign the resonances for each protons in ^1H NMR spectrum. The ^{19}F NMR spectrum showed mainly two peaks at δ 12.97 & 12.96 ppm. Mass calcd for $C_{60}H_{58}N_4F_{12}O_{10}$: 1223.13. Found: 1223.30

Method for in vitro biological studies:

The *in vitro* photosensitizing activity of fluorinated photosensitizers **1-4,** chlorin **30** and bacteriochlorin **31** was determined in radiation induced fibrosarcoma (RIF) tumor cell lines.[18] The RIF tumor cells were grown in alpha-DMEM with 10% fetal calf serum, penicillin and streptomycin. Cells were maintained in 5% CO_2, 95% air and 100% humidity. For determining the PDT efficacy, these cells were plated in 96-well plates and a density of $1x10^4$ cells well in complete media. After overnight incubation, the photosensitizers were added at variable concentrations, washed once with PBS. Cells were then illuminated with a 1000W Quartz Halogen Lamp with IR and band pass dichroic filters to allow light between 400nm-700 nm, at a dose rate of 16mW/cm^2. The drug dose that produced optimal cell kill was determined. The photosensitizing efficacy of other photosensitizers was then determined under similar experimental conditions. After PDT, the cells were washed once and placed in complete media and incubated for 48 hours. The 10ml of 5.0mg/ml solution of 3-[4,5-dimethylthiazol-2-yl]-2,5-

diphenyltetrazoliumbromide dissolved in PBS (Sigma, St. Louis, MO) was added to each well. After one hour incubation at 37^0C the MTT and media were removed and 100 ml DMSO was added to solubilize the formazin crystals. The 96-well plate was read on a microtiter plate reader (Miles Inc. Titertek Multiscan Plus MK II) at an absorbance of 560 nm. The results were plotted as percent survival of the corresponding dark (drug no light) control for each compound tested. Each data point represents the mean from 3 separate experiments, and the error bars are the standard deviation. Each experiment was done with 5 replicate wells.

Photophysical Measurements.

Absorption spectra were recorded on a Hewlett Packard 8453A diode array spectrophotometer. Time-resolved fluorescence and phosphorescence spectra were measured by a Photon Technology International GL-3300 with a Photon Technology International GL-302, nitrogen laser/pumped dye laser system, equipped with a four channel digital delay/pulse generator (Stanford Research System Inc. DG535) and a motor driver (Photon Technology International MD-5020). Excitation wavelengths were from 538 to 551 nm using coumarin 540A (Photon Technology International, Canada) as a dye. Fluorescence lifetimes were determined by a two-exponential curve fit using a microcomputer. Nanosecond transient absorption measurements were carried out using a Nd:YAG laser (Continuum, SLII-10, 4-6 ns fwhm) at 355 nm with the power of 10 mJ as an excitation source. Photoinduced events were estimated by using a continuous Xe-lamp (150 W) and an InGaAs-PIN photodiode (Hamamatsu 2949) as a probe light and a detector, respectively. The output from the photodiodes and a photomultiplier tube was recorded with a digitizing oscilloscope (Tektronix, TDS3032, 300 MHz). The transient spectra were recorded using fresh solutions in each laser excitation. All experiments were performed at 298 K.

For the $^1O_2$ phosphorescence measurements, an O_2-saturated C_6D_6 solution containing the sample in a quartz cell (optical path length 10 mm) was excited at λ = 532 nm using a Cosmo System LVU-200S spectrometer. A photomultiplier (Hamamatsu Photonics, R5509-72) was used to detect emission in the near infrared region (band path 1 mm).

Electrochemical and Spectroelectrochemical Measurements.

Cyclic voltammetry (CV) measurements were performed at 298 K on an EG&G Model 173 potentiostat coupled with an EG&G Model 175 universal programmer in deaerated benzonitrile solution containing 0.10 M TBAP as a supporting electrolyte. A three-electrode system was utilized and consisted of a glassy carbon working electrode, a platinum wire counter electrode and a saturated calomel reference electrode (SCE). The reference electrode was separated from the bulk of the solution by a fritted-glass bridge filled with the solvent/supporting electrolyte mixture. Thin-layer spectroelectrochemical measurements of the one-electron oxidized and one-electron reduced bacteriochlorin derivatives were carried out using an optically transparent platinum thin-layer working electrode and a Hewlett-Packard model 8453 diode array spectrophotometer coupled with an EG&G Model 173 universal programmer.

Acknowledgments

This research was supported by grants from DOD (???), NIH (CA 55792) , ???? (SK), (??? (KK) and the shared resources of the Roswell Park Cancer Center Support Grant (P30CA16056). We thank Beverly Chamberlin, Michigan State University, East Lansing for mass spectrometry results. The elemental analyses were performed at Midwest Microlab, Indianapolis.

References.

1. (a) Pandey, R. K.; Zheng, G. In the Porphyrin Handbook; Smith, K. M.; Kadish, K.; Guilard, R. Eds.; Academic Press, San Diego, 2000. (b) Dougherty, T. J.; Gomer,

C.;Henderson, B. W.; Jori, G.; Kessel, D.; Kobrelik, M.; Moan, J.; Peng, Q. *J. Natl. Cancer Inst.* **1998**, *90*, 889. (c) Bonnett, R. *J. Heterocyclic Chemistry*, **2002**.

2. Sherman, W. M.; Allen, C. M.; van Lier, J. E. *Methods Enzymol.* **2000**, *319*, 376.
3. Workman, P.; Maxwell, R. J.; Griffiths, J. R. *NMR Biomed.* **1992**, *5*, 270-272.
4. Bottomly, P. A. Human in vivo spectroscopy in diagnostic medicine: Clinical tool or research probe? *Radiology,* **1989**, *170*, 1.
5. Mason, R. P.; Shukla, H.; Antich, P. P. *Magn. Reson,. Med.* **1993**, 29, 296.
6. ??????
7. Jameson, C. J. Fluorine (Ed. Mason, J.) Multinuclear NMR, Chapter 16, Plenum, New York, **1987**, 437.
8. Japanese
9. Barton, D. H. R.; Zard, S. Z. J. *Chem. Soc. Chem. Commun.* **1985**, 1098.
10. Caveleiro, J. A. S.; Gonsalves, A. M. d'A. R.; Kenner, G. W.; Smith, K. M. *J. Chem. Soc. Perkin Trans.* **1973**, 240.
11. Jackson, A. H.; Smith, K. M. in the Total Synthesis of Natural Products, ed. J. *ApSimon, Wiley, New York*, **1973**, vol. 3, pp. 144 and **1984**, vol. 6, pp. 23.
12. Arsenault, G. P.; Bullock, E. and MacDonald, S. F. *J. Am. Chem. Soc.* **1960**, *82*, 4384.
13. Clezy, P. S.; Fookes, C. J. R.; Liepa, A. J. *Aust. J. Chem.* **1977**, *30*, 2017.
14. (a) Pandey, R. K.; Jackson, A. H.; Smith, K. M. *J. Chem. Soc. Perkin Trans I,* **1991**, 1211. (b) Smith, K. M.; Pandey, R. K. *Tetrahedron Lett.* **1986**, *27*, 2717. (c) Jackson, A. H.; Pandey, R. K.; Rao, K. R. N. and Roberts *E. Tetrahedron Lett.* **1985**, 793.
15. K. M. Smith in *"The Porphyrins and Metalloporphyrins"* (Ed. K. M. Smith), Elesvier Sci. Amsterdam. **1975**.
16. Fukuzumi, S.; Suenobu, T.; Patz, M.; Hirasaka, T.; Itoh, S.; Fujitsuka, M.; Ito, O. *J. Am. Chem. Soc.* **1998**, *120*, 8060.
17. Electrochemical
18. (a) Pandey, R. K.; Sumlin, A. B.; Potter, W. R.; Bellnier, D. A.; Henderson, B. W.; Constantine, S.; Aoudia, M.; Rodgers, M. A. J.; Smith, K. M.; Dougherty, T. J. *Photochem. Photobiol.* **1996**, *63*, 194. (b) Henderson, B. W.; Bellnier, D. A.; Graco, W. R.; Sharma, A.; Pandey, R. K.; Vaughan, L.; Weishaupt, K. R.; Dougherty, T. J. *Cancer Res.* **1997**, *57*, 4000. (c) Zheng, G.; Potter, W. R.; Camacho, S. H.; Missert, J. R.; Wang,

G.; Bellnier, D. A.; Henderson, B. W.; Rodgers M. A. J.; Dougherty, T. J. and Pandey, R. K. *J. Med. Chem.* **2001**, *44*, 1540.

19. (a) Kessel, D.; Luo, Y. *Cell Diff.* **1999**, *6*, 28. (b) Verma, A.; Facchina, S. L.; Hirsch, D. J.; Song, S. Y.; Dillahey, L. F.; Williams, J. R.; Snyder, S. H. *Mol. Med.* **1998**, *4*, 40.

20. Chen, Y.; Graham, A.; Potter, W.; Morgan, J.; Vaughan, L.; Bellnier, D. A.; Henderson, B. W.; Oseroff, A.; Doughty, T. J. and Pandey, R. K. *J. Med. Chem.* **2002**, *45*, 255-258.

21. Li, Guolin; Graham, A.; Potter, W.; Grossman, Z. D.; Oseroff A.; Dougherty, T. J. and Pandey, R. K. *J. Org. Chem.* **2001**, *66*, 1316.

Table 1. Absorption maxima (Q-band), fluorescence emission maxima and fluorescence emssion lifetime in deaerated PhCN at 298 K, and phosphorescence emission maxima in deaerated 2-MeTHF at 77 K.

	λ_{max}(fluorescence) nm		τ(fluorescence) ns	λ_{max}(phosphorescence) nm
26	**628**	**693**	**18.5**	**822**
27	**627**	**693**	**17.9**	**822**
28	**628**	**693**	**17.3**	**822**
29	**628**	**692**	**17.6**	**823**
1	**628**	**693**	**18.6**	**823**
2	**627**	**692**	**16.1**	**823**
3	**628**	**693**	**18.5**	**822**
4	**628**	**691**	**17.7**	**822**
4a	**629**	**693**	**18.2**	**822**
30	**652**	**a**	**3.8**	**842**
31	**720**	**a**	**3.3**	**806**

[a] **shoulder**

Table 2. T-T absorption maxima, T-T decay rate constants in the absence and presence of oxygen, quenching rate constant of the triplet excited state by oxygen in PhCN, and quantum yield of singlet oxygen in C_6D_6.

	λ_{max}(T-T), nm	τ(T-T), μs	k_{EN}, $M^{-1}s^{-1}$	$\Phi(^1O_2)$
26	450	1.0 x 10	9.4×10^8	0.26
27	450	1.1 x 10	1.1×10^9	0.57
28	450	1.1 x 10	1.0×10^9	0.68
29	450	1.1 x 10	8.9×10^8	0.33
1	450	8.3	9.9×10^8	0.61
2	450	1.4 x 10	9.0×10^8	0.75
3	450	1.9 x 10	1.0×10^9	0.81
4	450	2.5 x 10	1.0×10^9	0.36
4a	450	2.3 x 10	9.7×10^8	0.27
30	440	1.9×10^2	1.1×10^9	0.30
31	440	7.7 x 10	1.1×10^9	0.31

Table 3. Half-wave Potentials (V vs SCE) of Fluorinated and Non-fluorinated Porphyrins, in PhCN containing 0.1 M TBAP.

group	compound	ox				red		HOMO -
		4th	3rd	2nd	1st	1st	2nd	LUMO
I								
	4			1.24[c]	0.88[c]	-1.29	-1.62	2.17
	2		1.37[a]	1.14[c]	0.88[c]	-1.38[d]	-1.77	2.26
	3			1.28[a,c]	0.90[c]	-1.40	-1.76	2.30
	1		1.40[a]	0.83[a]	0.73[a]	-1.43	-1.74	2.16
II	**4a**			1.24[c]	0.90[c]	-1.37	-1.74	2.27
	26			1.36[a]	0.85[a]	-1.44	-1.65	2.29
	27		1.24[a]	1.14[a]	0.96[a]	-1.44	-1.61	2.40
	29	1.28[a]	1.16[a]	0.94[a]	0.76[a]	-1.46[b,f]	-1.63	2.22
III								
	30		1.48[a]	1.16[a]	0.74	-1.30	-1.71	2.04
	31	1.16[a]	1.03[a]	0.71	0.50	-1.46[e]	-1.81	1.96

[a] E_{pa} at scan rate 0.1 V/s.

[b] E_{pc} at scan rate 0.1 V/s.

[c] at scan rate 0.5 V/s.

[d] A small peak at E_{pc} = -0.61 V also can be observed.

[e] A peak at E_{pc} = -1.29 V also can be observed.

[f] Two small peaks at E_{pc} = -0.52 V and E_{pc} = -0.94 V also can be observed.

Table 4a. UV-visible Data of Fluorinated and Non-fluorinated Porphyrins, in PhCN containing 0.1 M TBAP.

group	compound	λ_{max}, nm (ε x 10^{-4}, $M^{-1}.cm^{-1}$)				
		Soret band	visible	bands		
I						
	4	408(12.71)	503(1.13)	536(0.51)	572(0.47)	626(0.19)
	2	409(11.23)	503(0.74)	538(0.60)	572(0.74)	624(0.29)
	3	407(7.25)	503(0.65)	535(0.30)	571(0.27)	625(0.10)
	1	407(13.12)	503(1.29)	535(0.62)	572(0.58)	625(0.28)
II	**4a**	408(11.96)	503(1.22)	536(0.60)	572(0.55)	625(0.25)
	26	407(16.20)	504(1.24)	536(0.27)	573(0.23)	624(0.09)
	27	407(12.47)	503(0.48)	535(0.20)	572(0.16)	624(0.10)
	29	412(12.70)	504(0.57)	538(0.74)	570(0.95)	615(0.21)
	28	407(9.58)	503(0.88)	535(0.40)	572(0.37)	624(0.15)
III						
	30	402(8.28)	501(0.79)	548(0.17)	593(0.26)	648(2.12)
	31	399(8.90)	506(1.28)	593(0.35)	645(2.02)	715(1.70)

Table 4b. UV-visible Data of Fluorinated and Non-fluorinated Porphyrin Reduction Products in PhCN, containing 0.2 M TBAP.

group	compound						
I							
	[4]$^-$	413(7.11)	788(3.40)				
	[2]$^-$	408(5.69)	437(3.68)s	578(0.74)	694(0.69)	813(0.89)	
	[3]$^-$	407(4.31)	503(0.49)	534(0.26)	568(0.23)	796(0.89)	
	[1]$^-$	409(6.05)	432(4.86)s	578(0.49)	700(0.57)	807(0.73)	
II	**[4a]$^-$**	413(4.86)	435(5.51)	578(0.44)	795(0.70)		
	[26]$^-$	410(6.77)	434(6.30)	578(0.21)	792(0.34)		
	[27]$^-$	409(5.14)	437(4.09)	502(0.37)	800(0.49)		
	[29]$^-$						
	[28]$^-$	408(5.21)	439(2.50)s	503(0.72)	576(0.33)	688(0.33)	800(0.44)
III							
	[30]$^-$	402(3.54)	499(0.65)	535(0.65)	649(1.04)	735(1.15)	
	[31]$^-$	406(6.75)	499(1.10)	576(0.64)	649(1.22)	827(0.77)	

Figure Captions

Figure 1. Fluorescence spectrum of **3** (7.3×10^{-6} M) in PhCN at 298 K.

Figure 2. Fluorescence decay of **3** (7.3×10^{-6} M) in deaerated PhCN at 298 K by excitation 548 nm at $\lambda_{em} = 626$ nm.

Figure 3. T-T absorption spectrum of **3** (7.3×10^{-6} M) obtained by the laser flash photolysis in deaerated PhCN at 4.0 μs after laser excitation (355 nm) at 298 K.

Figure 4. Kinetic trace for the T-T absorption of **3** (7.3×10^{-6} M) at 450 nm in deaerated PhCN. Inset: First-order plot.

Figure 5. Cyclic voltammegram of **3, 4, 4a**, **26**, **30** and **31** in PhCN containing 0.1 M TBAP.

Figure 6. The UV-visible spectral changes of **3** upon the first reduction at -1.50 V and the first oxidation at +1.10 V in PhCN containing 0.2 M TBAP.

Figure 7. The UV-visible spectral changes of **30** upon the first reduction at -1.50 V and the first oxidation at +0.90 V in PhCN containg 0.2 M TBAP.

Figure 8. The *in vitro* photosensitizing activity of various fluorinated photosensitizers in RIF tumor cells at a concentration of 1.0 μmol. **(A):** Fluorinated porphyrins **1-3**. **(B)** Fluorinated porphyrin 4 and the corresponding dihydroxychlorin **30** and the tetrahydroxybacteriochlorin **31**. Control: Cell exposed to light without photosensitizer or cells with photosensitizer but no light exposure.

Figure 9: Comparative intracellular localization of fluorinated porphyrin **4** and the related chlorin **30** and bacteriochlorin **31**.

Figure 1

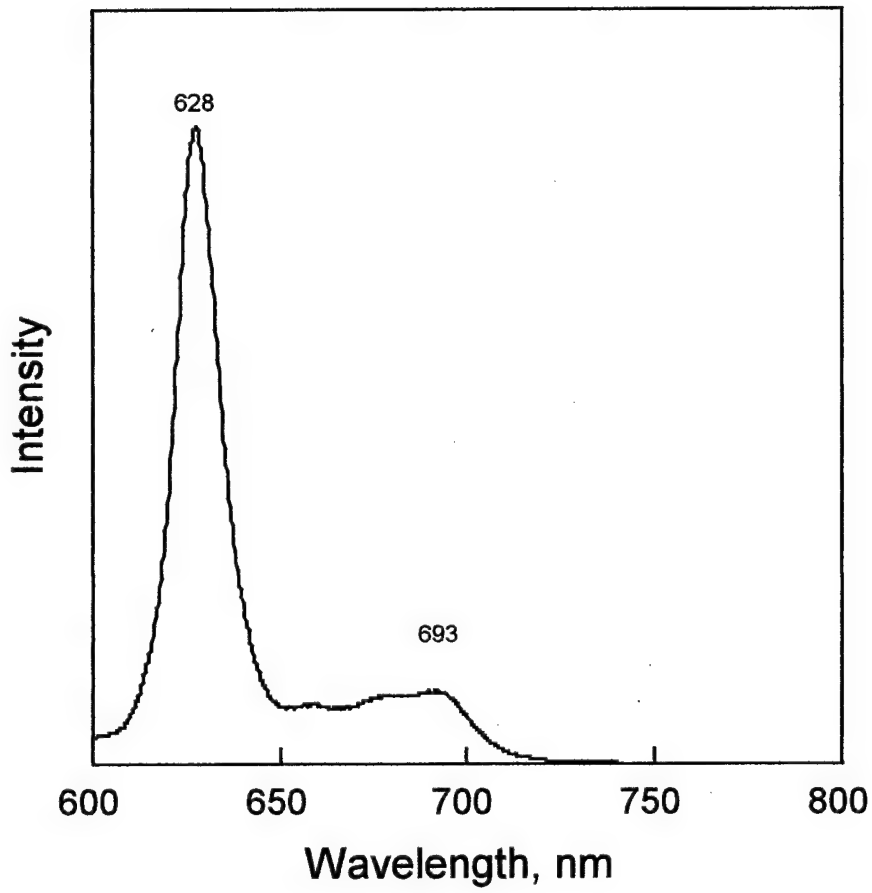

Figure 2

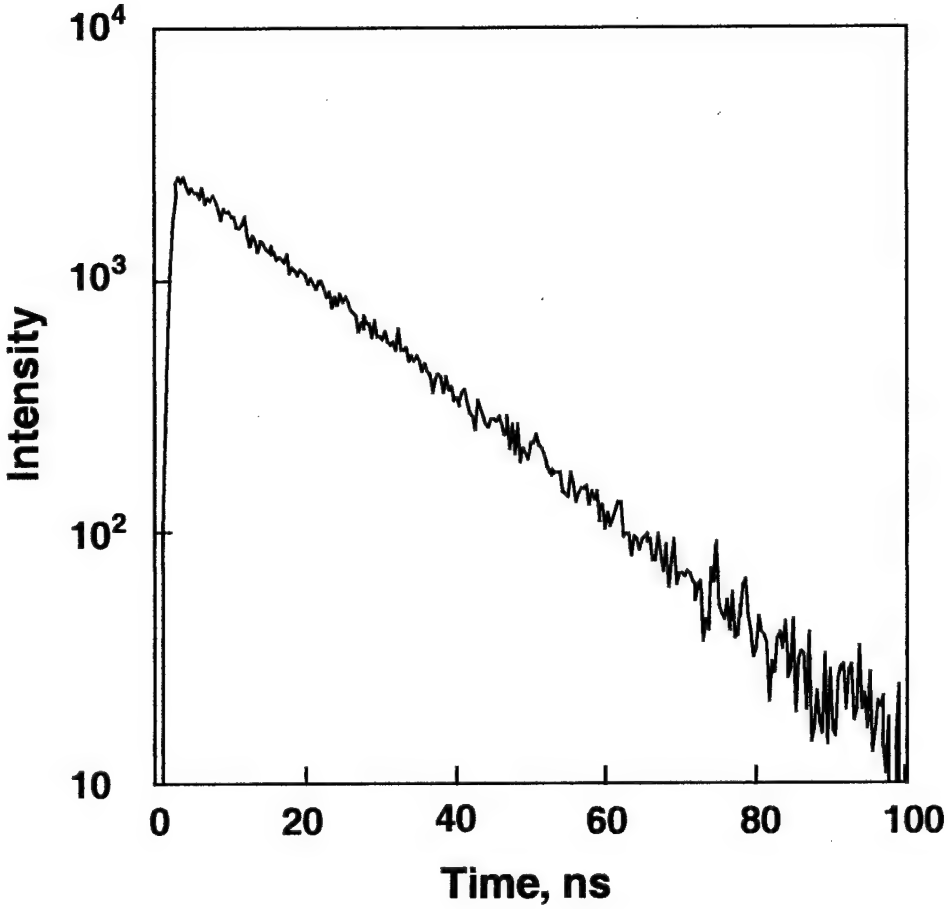

Figure 3

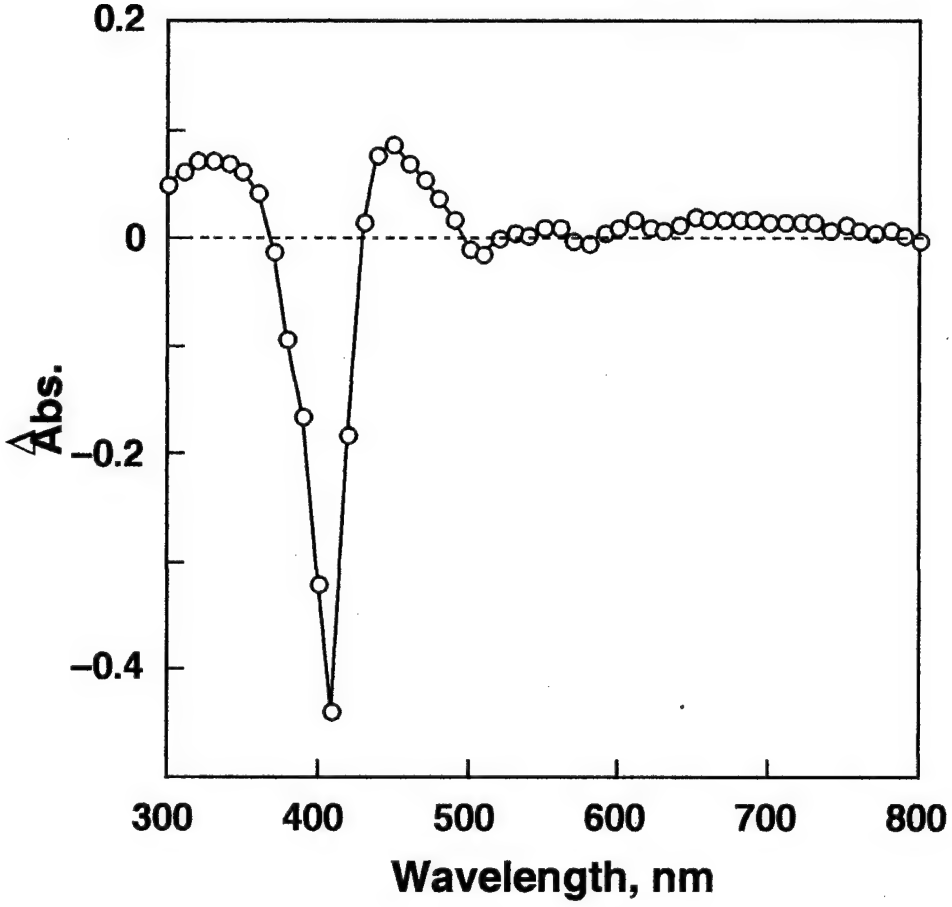

Figure 4

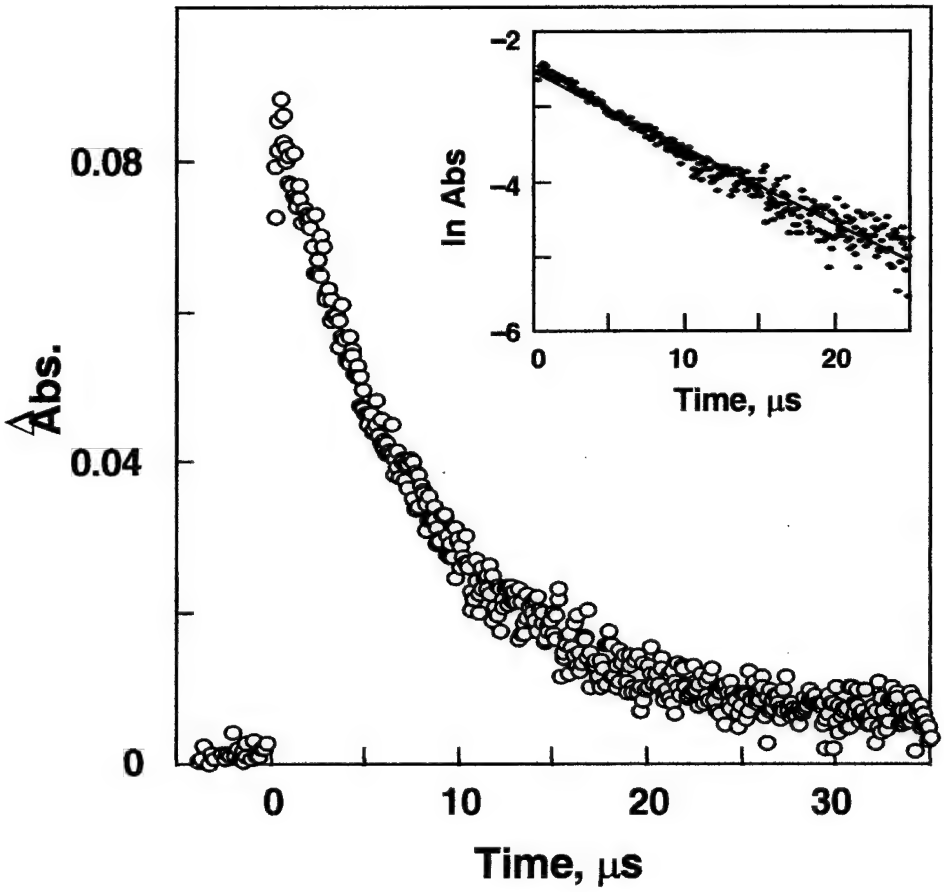

Figure 5

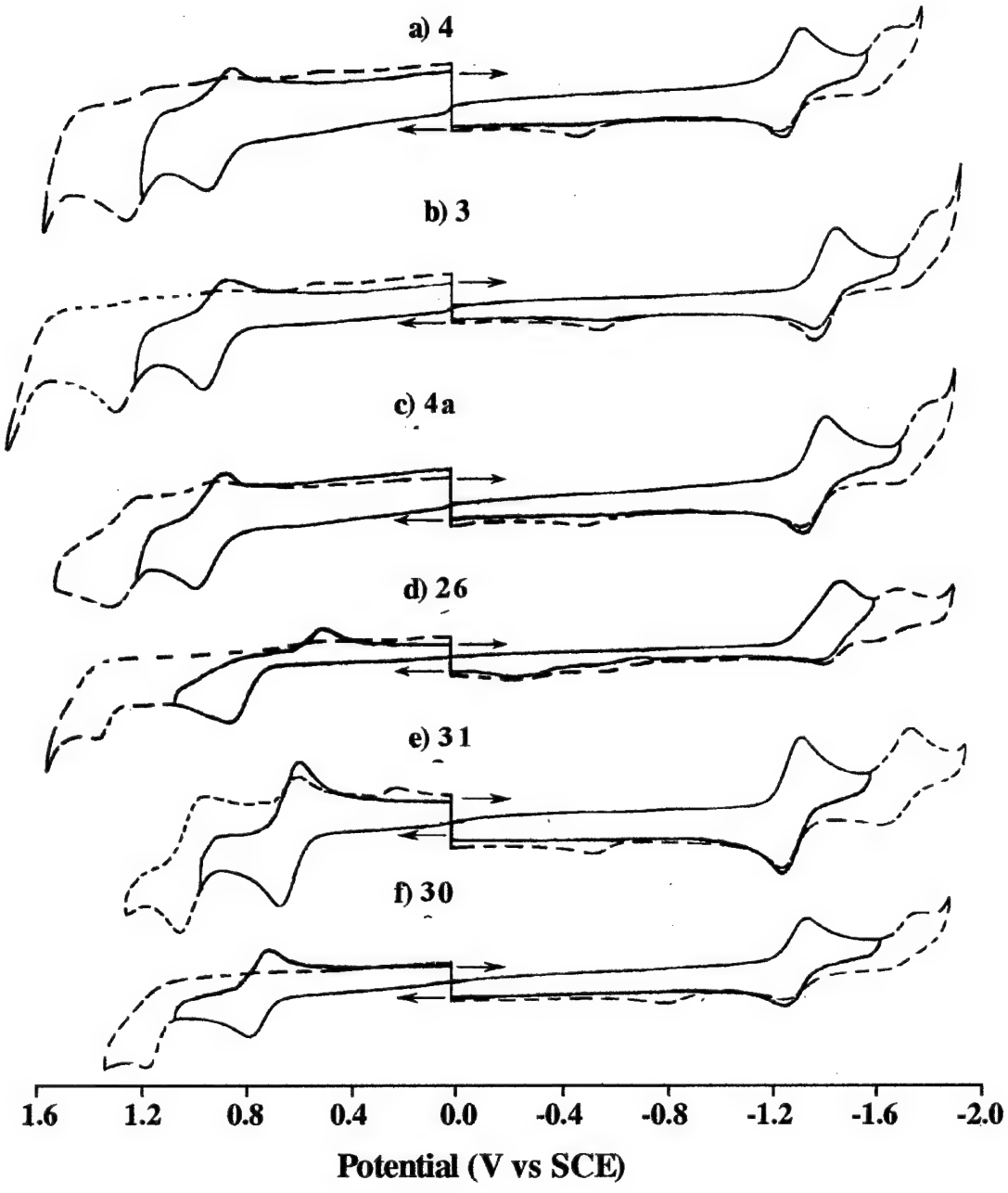
a) 4
b) 3
c) 4a
d) 26
e) 31
f) 30
1.6
1.2
0.8
0.4
0.0
-0.4
-0.8
-1.2
-1.6
-2.0
Potential (V vs SCE)

Figure 6

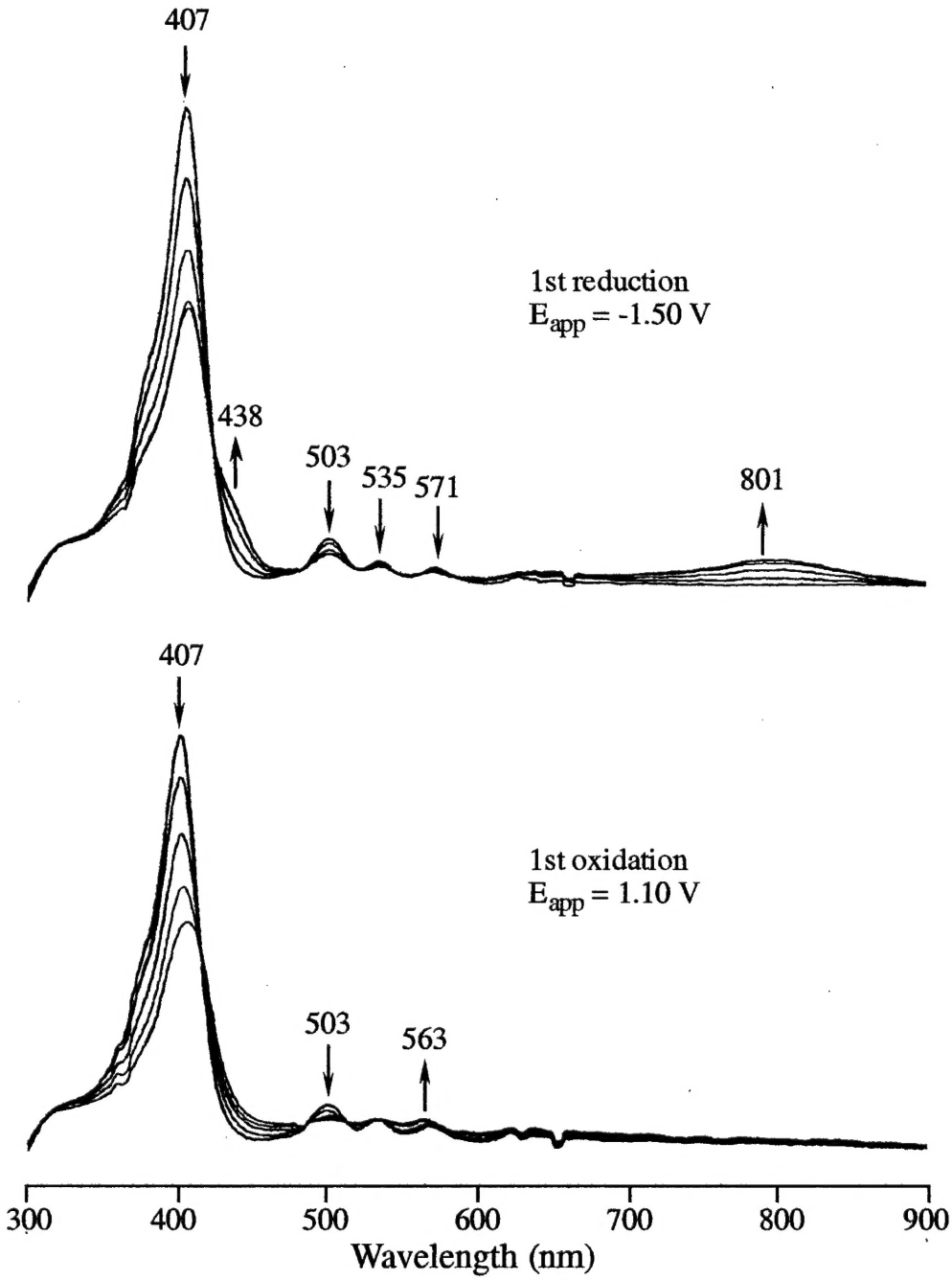
407
1st reduction
E_{app} = -1.50 V
438
503
535
571
801
407
1st oxidation
E_{app} = 1.10 V
503
563
300
400
500
600
700
800
900
Wavelength (nm)

Figure 7

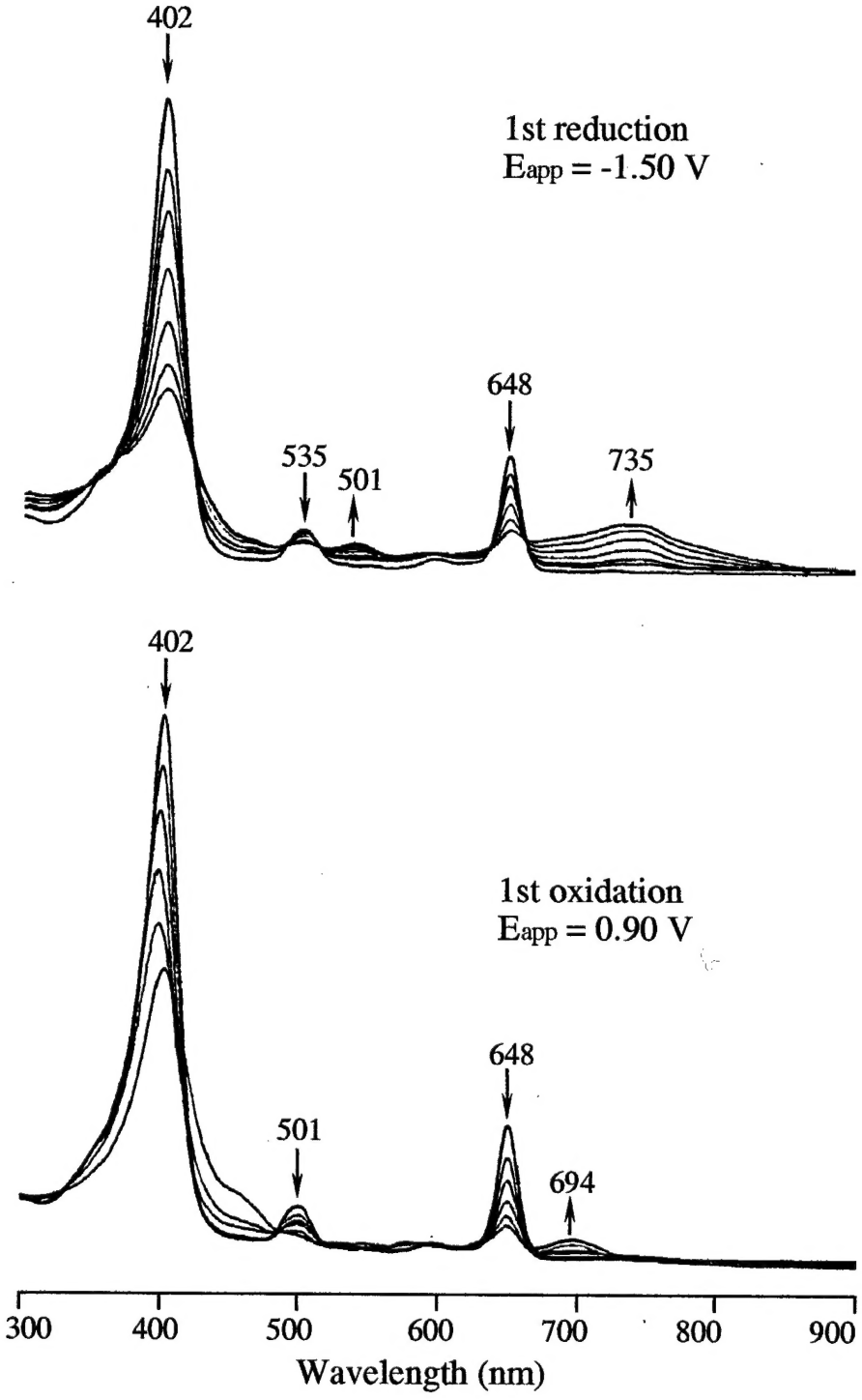
402
1st reduction
Eapp = -1.50 V
648
535
501
735
402
1st oxidation
Eapp = 0.90 V
648
501
694
300
400
500
600
700
800
900
Wavelength (nm)

Figure 8

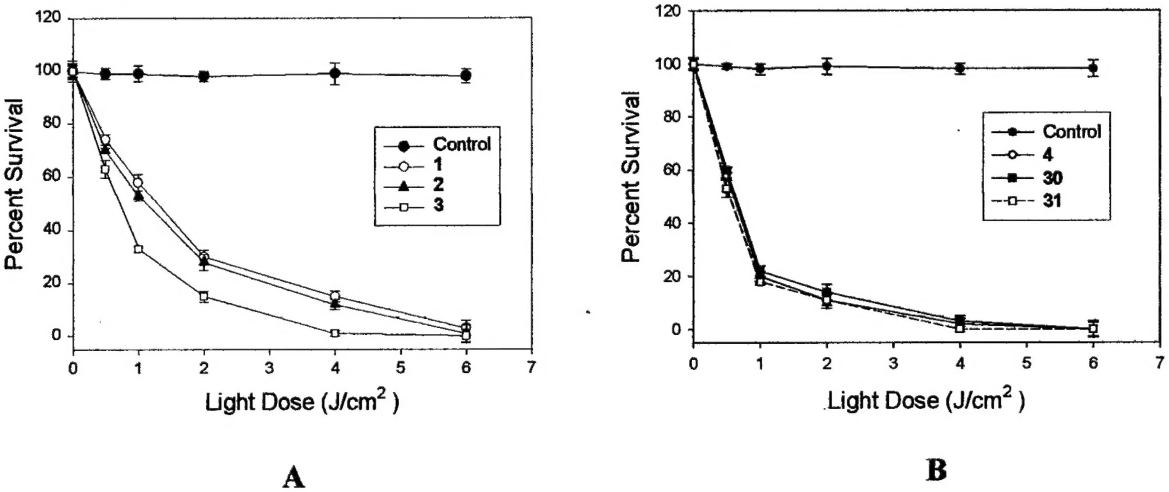

Figure 8: *In vitro* photosensitizing efficacy of various fluorinated photosensitizers in RIF tumor cells at a concentration of 1.0 μmol. **(A)**: Fluorinated porphyrins **1-3. (B)**: Fluorinated porphyrin **4** and the corresponding dihydroxychlorin **30** and tetrahydroxy bacteriochlorin **31**. Control: Cell exposed to light without photosensitizer and cells with photosensitizers but no light exposure.

Figure 9

Intracellular Localization

Fluorinated Chlorin 30

Rhodamine-123

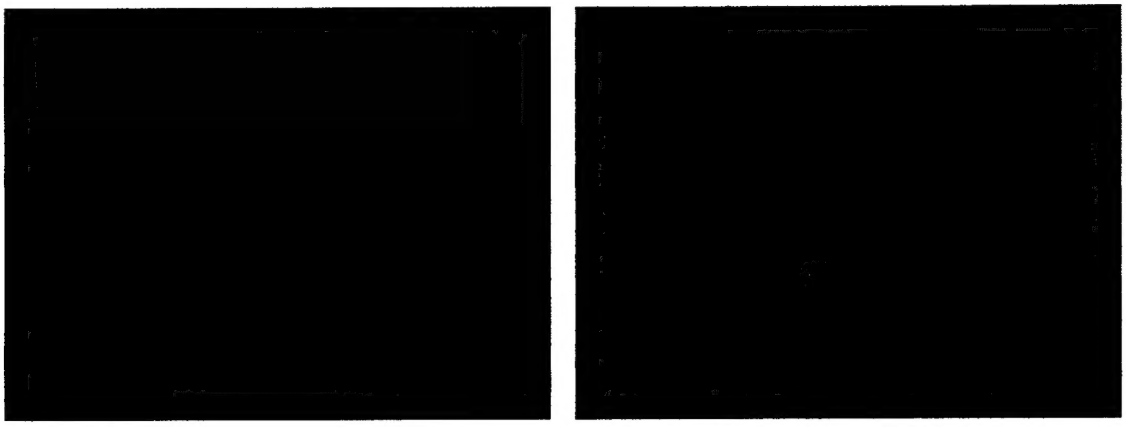

Overlay

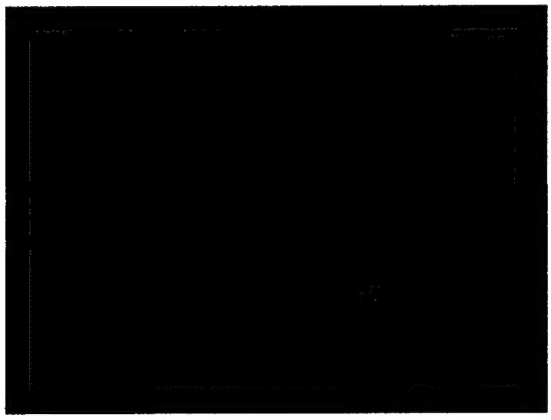

Figure 9: Comparative intracellular localization of fluorinated photosensitizer 30 and Rhodamine-123 in RIF tumor cells at 24 hours.